2010-01-01

Hydrological Characteristics Of A Large-Scale Flooding And Draining Experiment, Barrow, Alaska

Edith Jaurrieta De Velasco
University of Texas at El Paso, lady.edith@gmail.com

HYDROLOGICAL CHARACTERISTICS OF A LARGE-SCALE FLOODING AND DRAINING EXPERIMENT, BARROW, ALASKA

EDITH JAURRIETA DE VELASCO

Environmental Science Program

APPROVED:

Craig E. Tweedie, Ph.D.

Richard Langford, Ph.D.

Wen-Yee Lee, Ph.D.

Patricia D. Witherspoon, Ph.D.
Dean of the Graduate School

HYDROLOGIC CHARACTERISTICS WITHIN A DRAINED THAW LAKE BASIN, BARROW, ALASKA

by

EDITH JAURRIETA DE VELASCO, B.A., B.S.

THESIS

Presented to the Faculty of the Graduate School of

The University of Texas at El Paso

in Partial Fulfillment

of the Requirements

for the Degree of

MASTER OF SCIENCE IN ENVIRONMENTAL SCIENCE

Department of Environmental Science

THE UNIVERSITY OF TEXAS AT EL PASO

December 2010

Acknowledgements

First of all, thank you God and my family, for supporting me during these trying times of juggling parenthood with student life. ***(Primero que nada, gracias a Dios y a mi familia por todo el apoyo que me brindaron en estos momentos de lucha para tener éxito como madre y estudiante.)***

- Thanks to all 2005-2008 field assistants from the Systems Ecology Lab who made data collection possible and helped me out when I had questions or doubts.
- Thanks to BASC for logistic support, UIC for BEO land use permit, the US National Science Foundation for their financial support (Grant no. 0421588), and PND Incorporated for collecting and processing LiDAR data and providing technical advice on further processing of LiDAR data set.
- Thanks to my academic advisors and mentors for working with me to turn in a final product: Dr. Craig Tweedie, Dr. Richard Langford, Dr. Wen Ye Lee, and Dr. Jose Hurtado, Dr. Andre Ellis, and Dr. Aaron Velasco.

Abstract

The Arctic appears to be affected by climate change more so than any other region on Earth. Some of the most significant climate change impacts reported for the Arctic are associated with dramatic shifts in the hydrologic regime of terrestrial ecosystems. Understanding the hydrologic processes that are associated with different components of arctic terrestrial ecosystems is important because water in the form of snow or rain influences a range of properties and processes such as land-atmosphere energy and trace gas fluxes, nutrient cycling, ecosystem dynamics, biodiversity, periglacial processes and surface albedo. Furthermore, plants, animals, and native people of the Arctic depend on these ecosystems and a substantial hydrologic shift could significantly impact provision of ecosystem goods and services and, therefore, natural system and human well being.

A climatic warming and drying trend has been observed in Northern Alaska, near the Iñupiat Village of Barrow as well as elsewhere in the Arctic. Importantly, there remains a great deal of uncertainty as to how coastal tundra ecosystems will respond to such a trend. To assist in addressing this uncertainty, a large-scale, multi-investigator flooding and draining experiment was initiated in summer 2005, and plot to landscape responses of multiple parameters (i.e. soil moisture, plant phenology, and trace gas flux) were measured. The experimental area was situated on the Barrow Environmental Observatory in a vegetated drained thaw-lake basin (DTLB) that was divided into three treatment areas: an experimentally flooded section, an experimentally drained section, and a control section that was not flooded or drained. For this thesis, baseline hydrology data were gathered between 2005 and 2007, prior to the initiation of the flooding and draining experiment. Measurements were continued in 2008 but under experimental conditions (+/- 10 cm flooding/draining respectively). The overarching goal of

this thesis is to characterize baseline hydrologic conditions in the experimental DTLB as a contribution to the Biocomplexity Initiative sponsored by the US National Science Foundation.

Climate data from the NOAA Earth Systems Research Lab, (Global Monitoring Division's online U.S. Climate Reference Network) were attained to plot summer climatic conditions at the study site for June-August of years 2005 through 2008. Average precipitation for all years was a few millimeters lower than the average 29 year precipitation reported by the NOAA and average temperature was virtually the same as the 29 year average. Data from an air-borne LIght Detection And Ranging (LiDAR) survey were processed with ArcGIS 9.2 Geographic Information System (GIS) software to develop a Digital Elevation Model (DEM) of the experimental area. ArcHydro, an extension to ArcGIS, was used to locate research infrastructure such as the dikes and model the catchment and drainage network of the study area. Snow depth measurements were taken along a 100m grid in the experimental DTLB. Snow depths were then converted to snow water equivalent measurements (SWE). Averaged over all years, snow depth and SWE fell within the range of other snow depth and SWE measurements in the Barrow region. Seasonal water table depth and thaw depth were collected in each experimental treatment and analyzed, using the statistical software JMP 8, to identify inter-annual and treatment differences. Following initiation of the manipulation, significant differences between the treatments were observed for thaw depth and water table depth. Water table depth was highest (close to the ground surface) in the flooded treatment and lowest (deepest underground) in the control treatment for summer 2007. In 2008, water table was highest in the flooded treatment, but lowest in the drained treatment. Maximum thaw depth occurred in the flooded treatment for summers 2007 and 2008. Minimum thaw depth was recorded in the control treatment in 2007 and the drained treatment in 2008. Confidence curves

fit to normalized seasonal time series of pond water levels indicate that ponds, in general, behaved in a uniform manner. A pre and post test of water levels in their respective treatment sections reveals that differences in water levels between each treatment for summers 2005-2008 were not significant. HOBO water level loggers were used to record pond temperature and the average temperature from all ponds was within range of pond temperatures recorded in the 1960's and 1970's. Meyer's evaporation equation was used to calculate evaporation. Results were a few millimeters higher than other evaporation rates for the region. This suggests evaporation may be the primary control on surface hydrology in ponds within the experimental area.

Continued long-term monitoring of hydrologic variables such as the ones observed in this thesis is important because natural and anthropogenic disturbances to hydrology can alter drainage patterns, geomorphic processes, vegetation structure and function, and land-atmoshphere feedbacks. This thesis documented substantial inter-annual variability and long term observations are likely to be needed to determine long term trends.

Table of Contents

List of Tables

List of Figures

Chapter 1: Introduction

More so than most other places on Earth, the Arctic is experiencing the impacts of climate change and feedbacks from this change have the potential to dramatically alter the Earth System (ACIA 2005, IPCC 2007). The effects of increasing surface air and ocean temperatures coupled with shifting climate patterns in the Arctic are causing sea ice extent and thickness to diminish (Richter-Menge *et al.* 2006, Richter-Menge *et al.* 2008), leaving the Arctic coastline vulnerable to more intense storm systems and increased coastal erosion (Aguirre *et al.* 2008). Arctic terrestrial ecosystems are also changing (Hinzman *et al.* 2005) - snowpack extent and duration is decreasing, river discharge is increasing (Richter-Menge *et al.* 2008), shrubs are expanding (Sturm M. 2001), and consequently, albedo is decreasing (Chapin *et al.* 2005). Circum-arctic thaw lakes and ponds are drying (Yoshikawa & Hinzman 2003, Smol & Douglas 2007) and permafrost is warming (Romanovsky *et al.* 2002). Furthermore, the exchange of important greenhouse gases such as carbon dioxide (CO2) and methane (CH4) in arctic tundra ecosystems may be changing Arctic climate (Serreze & Francis 2006, Christensen *et al.* 2008). Although long term changes have been recorded, there is a fundamental need to improve our understanding of connections and implications of cascading changes in physical, biological and human systems in the arctic and this will only be solved in process studies coupled to long term observations (SEARCH 2005).

A large amount of soil organic carbon is stored in the permafrost of the Alaskan Arctic Coastal Plain. The region also hosts an indigenous community, oil development, and is an important habitat for migratory birds, and other land animals, all of which are highly vulnerable to climate induced feedbacks that alter surface hydrology (Hinzman *et al.* 2005). The next

section of this thesis highlights the importance of hydrology to arctic terrestrial ecosystems near Barrow, Alaska and summarizes different arctic ecosystem components relevant to the overarching goal of this thesis, which is to better understand the hydrologic characteristics of a drained thaw lake basin that is the focus of a large-scale flooding and draining experiment.

1.1 Seasonal Hydrology and Energy Balance Dynamics of the Alaskan Arctic Coastal Plain

Land-atmosphere interactions in arctic coastal tundra ecosystems are strongly influenced by hydrology-related phenomena like precipitation (in the form of snow or rain), snowmelt runoff, evaporation, permafrost, and soil moisture (Lewellen 1972, Kane *et al.* 1992). The hydrologic cycle of the Arctic is very different to that of temperate regions in that snow can fall at any given time of the year due to persistent low air temperatures and the tundra is frozen for approximately nine months out of the year (Hobbie 1980). There is no sunlight from mid November to mid January; thereafter, the sun begins to gradually rise above the horizon and warms the land surface (Lewellen 1972). Albedo can be up to 85% during this time, thus little snowmelt occurs. Once albedo is lowered to 40% in late May, snowmelt increases and snow becomes saturated with water, initiating the spring runoff (Hobbie 1980).

On the north slope of Alaska, the spring runoff typically occurs around the first or second week of June and commonly persists for 5-10 days shortly before or during the summer solstice when the sun is highest on the horizon (Lewellen 1972, Kane *et al.* 1992). The spring runoff occurs laterally due to a low topographic gradient and ice-rich continuous permafrost which creates impermeable soils, leaving behind water-logged tundra above the permafrost (Engstrom *et al.* 2005, Woo *et al.* 2006). Once the ground is snow free, thawing begins and persists throughout the summer (Olsson *et al.* 2003). From June to August, the tundra begins to dry and

rates of evaporation increase to become a major component of water loss from tundra landscapes (Lewellen 1972, Bowling *et al.* 2003, Kane *et al.* 2008). Summer rain events and discharge can help recharge tundra soils (Lewellen 1972, Hinkel *et al.* 2001, Woo & Young 2006). Tundra landscapes of the arctic coastal plain, including ponds and wetlands, are important for sustaining biodiversity and are likely to be adversely affected by climate change (Jordan *et al.* 2007). Understanding hydrology-ecosystem interactions are important, for not only understanding the hydrological dynamics of the arctic coastal plain but also for predicting the likely impact of environmental change on biota (Hobbie 1975, Kane *et al.* 1992, Chapin 1993).

1.2 Repercussions of Climate Change on Arctic Terrestrial Ecosystems

Recent atmospheric warming and drying trends documented for Barrow, Alaska (Curtis *et al.* 1998, Stone *et al.* 2002, Hinzman *et al.* 2005) may be associated with regional hydrologic changes - for example, evapotranspiration (ET) compensating for reduced soil water content (Engstrom *et al.* 2005), and thaw depth altering water storage capacities and plant communities (Hinkel *et al.* 2001). The following sections describe geo- and biophysical processes that are linked to important climate change feedbacks affected by surface hydrology.

1.2.1 Permafrost and Periglacial Landforms

Permafrost is defined as any ground substrate that remains below 0º C for more than 2 years (US Arctic Research Commission Permafrost Task Force 2003, Schuur *et al.* 2008) . Permafrost exerts substantial control over surface energy budgets and the hydrology of coastal tundra and is largely responsible for the ubiquitous nature of wetlands, thaw lakes, and ponds as water is unable to penetrate the permafrost and remains perched above or near the surface of the ground (Engstrom *et al.* 2005). A relatively shallow layer called the active layer, above the

permafrost table, seasonally freezes and thaws and harbors most biophysical processes and activities (Kane *et al.* 1992, Ritter *et al.* 2002). The thickness of the active layer, known as thaw depth has been measured continuously in Barrow, Alaska since 1994 (Hinkel *et al.* 2001). A large amount of soil organic carbon, about 50kg/m3 is locked up in Arctic permafrost (Ping *et al.* 2008) and is equivalent to about 25% of the global soil organic carbon (Tarnocai & Broll 2008). Scientists speculate that if permafrost were to thaw significantly in the near future, microbial activity in the soils would heighten, thus increasing green house gas emissions to the atmosphere (US Arctic Research Commission Permafrost Task Force 2003). However, there is a possibility that the carbon locked up in the upper layers of these soils may continue to be sequestered with warming of the region because carbon could be transported further down into soils through cryoturbation, where the presence of permafrost would hinder microbial activity (Bockheim *et al.* 1999, Tarnocai & Broll 2008). The presence of ground ice in permafrost, coupled with freeze-thaw dynamics also plays a key role in non-glaciated or periglacial environments because they are associated with the interplay between periglacial landforms (Washburn 1980) and different land cover types in the region (Schuur 2008).

Ice wedges, low and high-centered polygons, ground ice, and frost boils are some of the periglacial landforms commonly found on the coastal plain of northern Alaska and are a product of frost action leading to cracking, subsidence, or uplifting of ground material (Fitzpatrick 1997, US Arctic Research Commission Permafrost Task Force 2003, Engstrom *et al.* 2005). Thermokarst terrain can also be found in periglacial environments and includes patterned ground like sorted and unsorted circles and drained-thaw lake basins (DTLB) (Washburn 1980). In the arctic, thermokarst degradation can result from the lateral erosion of ice-rich ground surfaces (i.e., coastal erosion) or vertical erosion where ground temperature and hydrologic pathways

have been altered (Ritter *et al.* 2002). These usually produce small ponds or lakes as water accumulates in small depressions, like low-centered polygons. These particular ponds can repeatedly breach and drain and/or coalesce with other ponds, producing a larger pond or a lake, hence the concept of the thaw lake cycle (Hobbie 1980). Smith et al. (2005) used remote sensing to note shifts in water storage capacities of small ponds and large lakes in Siberian tundra, concluding that small ponds are disappearing due to increased thermokarst activity. Significant geomorphic changes have also been observed in the Alaskan subarctic region, near Fairbanks (Jorgenson *et al.* 2001) and Council (Yoshikawa & Hinzman 2003), where suprapermafrost (above-permafrost) degradation is causing forest environments to fail and turn into wetlands. Such geomorphic change can negatively impact Arctic communities because of the potential damage to infrastructure that sits on top of warmer, more unstable permafrost (Nelson *et al.* 2002, US Arctic Research Commission Permafrost Task Force 2003). Smol and Douglas (2007), who witnessed the disappearance of Arctic ponds on Ellesmere Island's near Hershel, believe that high evaporation/precipitation (E/P) ratios have forced some water bodies to reach their ecological threshold, and hence their ubiquity in the Arctic may decline if warming continues in northern Arctic regions. This has yet to be documented for the Alaskan north slope and coastal plain.

1.2.2 Ecosystem Structure and Function

The low gradient microtopography of the north Alaskan coastal plain tundra coupled with snowmelt runoff produce lateral surface hydrologic pathways (Sturm *et al.* 2001, Woo & Guan 2006) that redistribute nutrients (Engstrom *et al.* 2005). Hobbie (1980) asserts that rainfall is more important than spring runoff in nutrient cycling because of soil and plant leaching. Precipitation as snow has decreased during the winter in the western Arctic (Curtis *et al.* 1998,

Stafford *et al.* 2000). It is difficult to assess whether summer rain will offset the lack of snowpack that has been observed and help supplement enough water and nutrients to the tundra or if the warming Arctic will result in a landscape change of wet-moist tundra to dry tundra, as noted in Hinzman et al., (2005).

In Alaska, the coastal tundra north of the Brooks Range is made up of dry and moist to wet tundra (Walker *et al.* 2005). Dwarf shrubs, sedges, and grasses grow to approximately 10-15 cm above the ground surface as a direct response to constant wind, low temperatures, and a shallow active layer (Hobbie 1975). Ecosystems with high soil moisture have low decomposition rates because anaerobic conditions reduces microbial activity, thereby improving capacities for carbon storage (Oechel *et al.* 1995), although these same conditions promote methanogenesis and methane as a powerful greenhouse gas (Zona & Oechel 2008).

1.2.3 Land-Atmosphere Interactions

Defining the hydrologic characteristics of the Alaskan arctic coastal plain is important because surface water and water in the active layer are linked to greenhouse gas fluxes, radiative forcing, soil moisture, nutrient cycling, and albedo (Judd & Kling 2002, Engstrom *et al.* 2005). Figure 1 shows a hydrologic gradient that commonly spans dry to aquatic tundra. Uptake of CO_2 by tundra can increase with increased soil moisture, especially in aquatic vegetation (Macrae *et al.* 2004, Oberbauer *et al.* 2007). Conversely, CH_4 uptake decreases in aquatic vegetation as soil moisture increases (Christensen *et al.* 2008, Zona *et al.* 2009). Of utmost concern are the total combined emissions of CO2 and CH4 that increase with increased soil moisture, thus creating a positive radiative forcing (IPCC 2007, Christensen *et al.* 2008). The radiative forcing potential increases rapidly because the capacity of CH_4 to warm the atmosphere is approximately 25 times greater than CO_2 over a 100 year time frame (Joabsson *et al.* 1999). Albedo decreases from dry

to wet tundra because the reflectivity of tundra vegetation is greater than the reflectivity of solar energy from standing water (Chapin 1993). Since climate models predict that precipitation will increase in some polar regions (ACIA 2005), there is concern over the radiative forcing potential and albedo coupled with water inputs to positively feedback to climate and exacerbate the warming conditions already present in arctic coastal regions (Callaghan *et al.* 2004c). Overall, the Arctic is a highly connected system where change in one component can affect change in another (Hobbie *et al.* 2000, McGuire *et al.* 2009), especially in relation to the close linkage between water and carbon cycles, and there is a challenge to consider all of these components in a systems context to predict future arctic scenarios that will affect the global climate system.

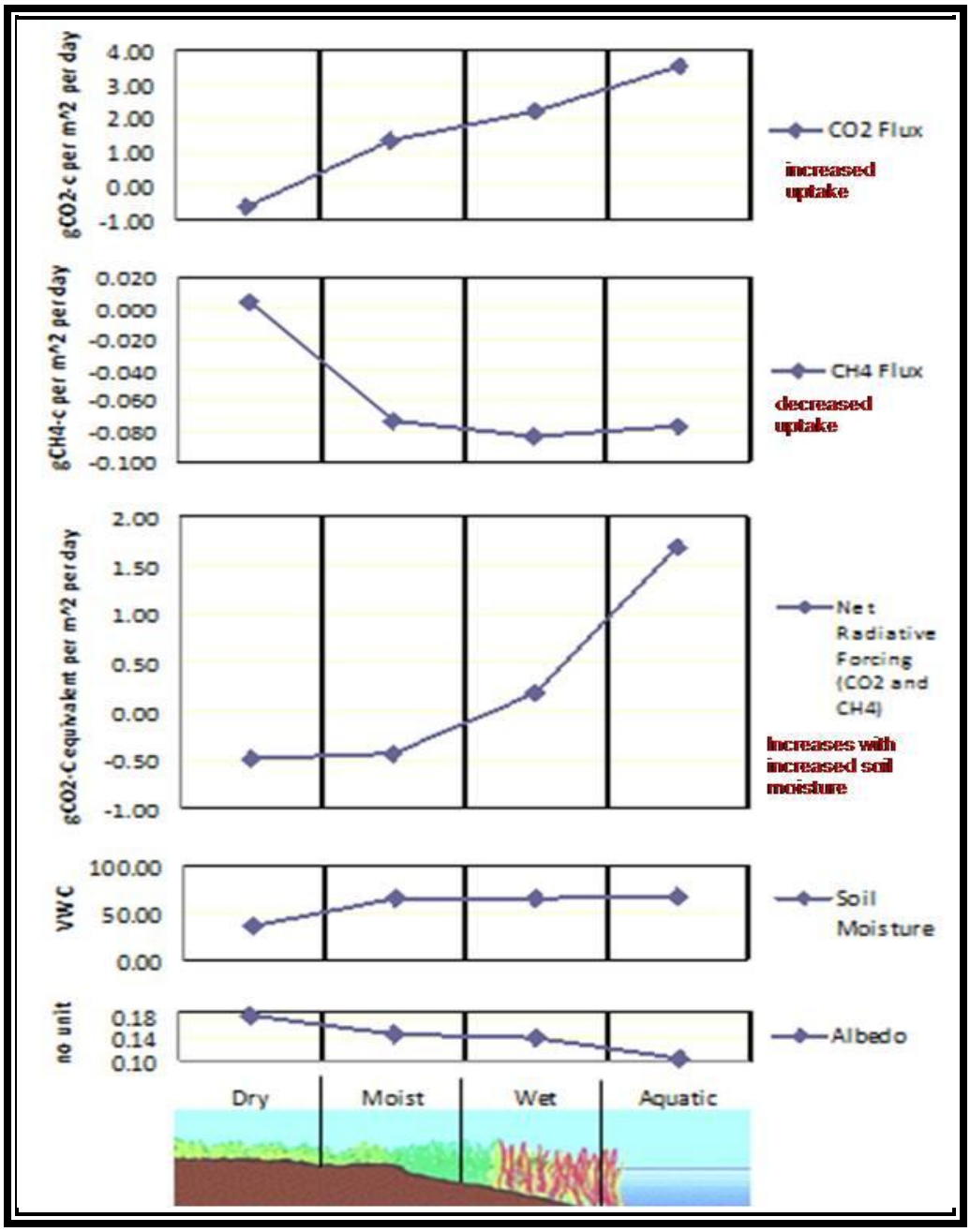

Figure 1. Land-atmosphere interactions in Arctic coastal tundra, shown at peak season (Lin, personal communication). As the soil water content increases from left to right, CO_2 uptake increases, whereas CH4 uptake decreases. The total combined emissions of these two greenhouse gases increases with soil moisture (net radiative forcing). Soil moisture increases, but stabilizes as water content increases. Albedo decreases as the reflectivity of ground vegetation is replaced with standing water.

1.3 Purpose of This Study

The purpose of this study is to better understand the hydrologic characteristics of a 60 hectare DTLB prior to and during the execution of a large-scale flooding and draining experiment that was funded under the Biocomplexity Initiative lead by the US National Science Foundation. The manipulation entails partitioning the DTLB into three sections: a northern section that was experimentally flooded, central section that was experimentally drained, and a southern section that was not manipulated to serve as a control. The flooded treatment will simulate a future wet tundra environment, since some climate models predict higher precipitation in arctic region The dry treatment will simulate a future dry Arctic tundra, which is what Arctic researchers have observed and expect as a continuing trend near Barrow, Alaska. Due to its size and logistic constraints associated with maintaining the experiment, it was not replicated, thus holding the control section relative to outside pond water levels is important for comparing between naturally-occurring wet and dry years. The flooding and draining was intended to be ±10cm of water, relative to the control section to account for inter-annual variability. The main focus of this thesis is to report on the multiple hydrologic characteristics existing at the study site as baseline data for future, more detailed eco-hydrologic studies.

Precipitation, temperature, snow depth, water table depth, thaw depth, pond water levels, and evaporation were compared to other studies within the Arctic coastal plain region to note any important changes or patterns. Another important task was to characterize the DTLB watershed and its drainage patterns. Pre and post analysis of the treatment effect on thaw depth, water table depth, and pond water levels was conducted to note any significant changes.

Chapter 2: Study Site Description

The coastal plain near Barrow, Alaska has been studied extensively since the 1940's, as per the bibliography compiled by Dr. Jerry Brown in the Arctic Research Consortium of the United States website – www.arcus.org (ARCUS 1999). The Barrow Environmental Observatory (BEO) – Figure 2, is a 7,466 acre preserve of Arctic coastal tundra, located adjacent to Elson Lagoon on the Beaufort Sea coast near the city of Barrow (71º19'53'', 156º34'4"). The land was set aside in the early 1990's by the Ukpeaġvik Iñupiat Corporation to facilitate long-term, year-round arctic research and collaboration between the scientific and local community (UIC 2003). The Barrow Arctic Science Consortium (BASC) manages the BEO through a working group that produces annual reports of current research activities – research bases, found under the BASC website, www.arcticscience.org.

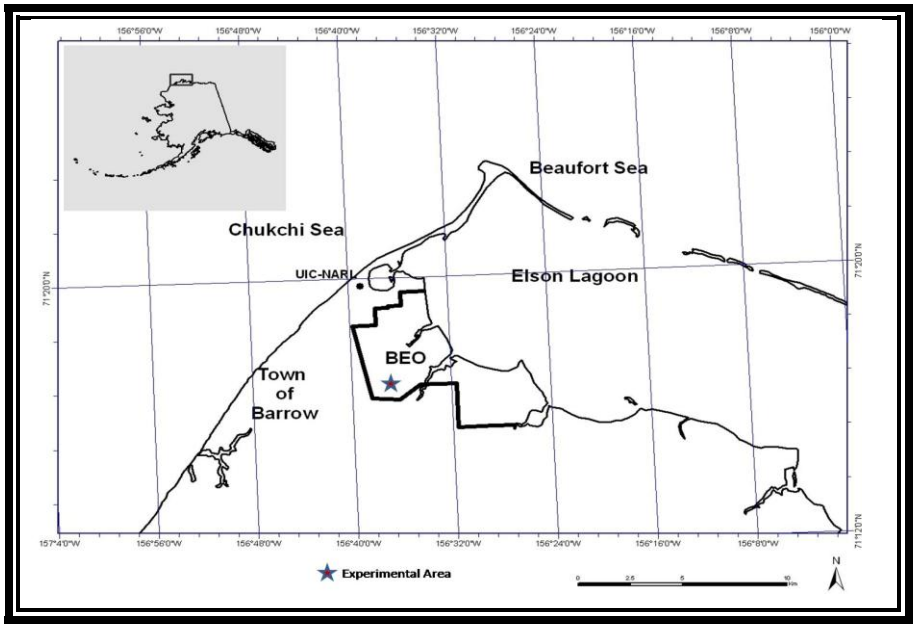

Figure 2. Map showing northernmost region of the United States. The bold, black outline indicates the Barrow Environmental Observatory (BEO). The star is the experimental area. To the left of the BEO is the town of Barrow, Alaska, and above the BEO is the research hub (UIC-NARL). ***Map courtesy of Systems Ecology Lab, University of Texas at El Paso (SEL, UTEP).***

2.1 Biocomplexity Experimental Infrastructure

The information described in section 2.1 is derived from the 2005-2007 Annual BEO reports, written by lead project investigators and compiled by the BEO subcommittee. Intense planning and permitting was required to accelerate placement of the biocomplexity infrastructure inside the BEO, with a "no harm to wildlife" guarantee and minimal damage to the tundra.

Figure 3 shows a map of the infrastructure developed for the BE. Initially, a matted trail was created to lessen damage from foot traffic on the tundra. These were replaced by elevated boardwalks in sections close to the drained lake basin in 2006. The Tommy Docks used for the construction of the elevated boardwalks allowed for boardwalks to be lowered or raised as needed, but required regular adjustments to accommodate differential settling of land as it thawed during the summer seasons. Three 200m long boardwalks inside the drained thaw lake basin (manipulation site) were constructed in 2005, but were extended to 300m in length in 2006. Each boardwalk is located in a treatment section of the hydrologic manipulation experiment. Boardwalks also provided easy access to sampling sites without causing excessive disturbance to the tundra.

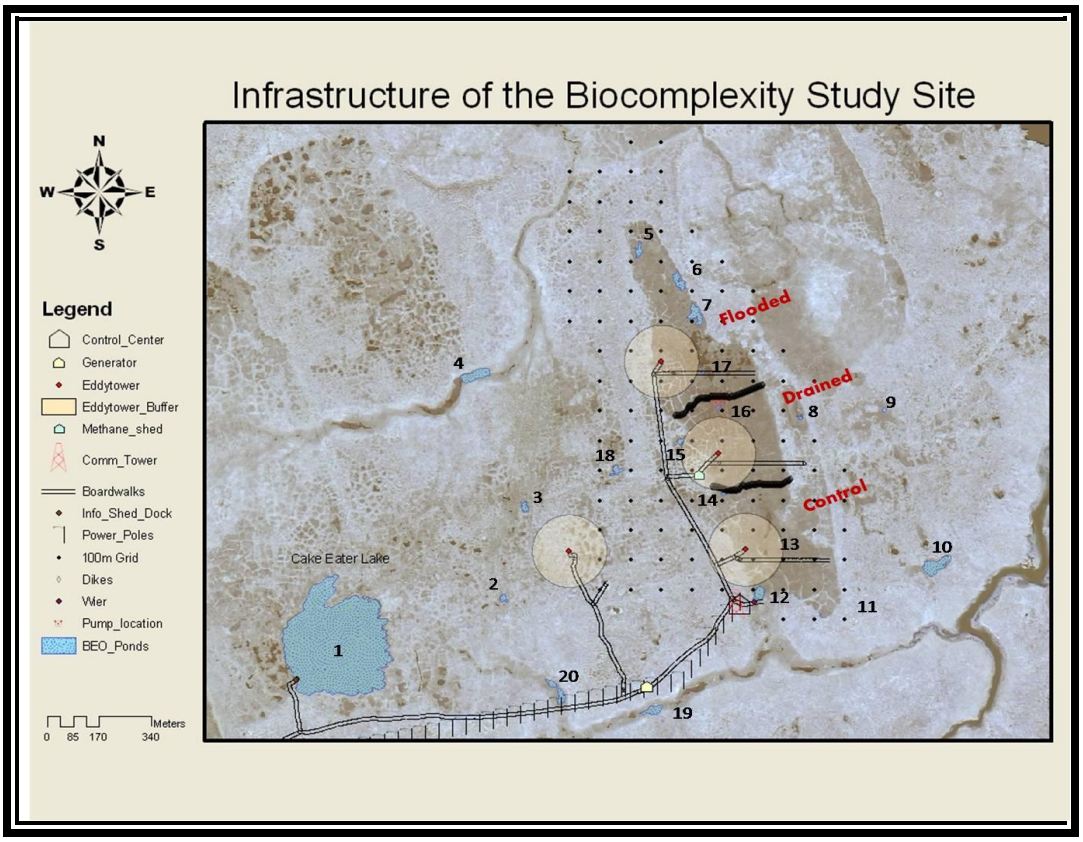

Figure 3. ***Infrastructure of the Biocomplexity study site and other experiments. Ponds colored blue were monitored prior and during the experimental manipulation. Additional information about the research activities that took place on the sites can be found at the Barrow Area Information Database – Internet Map Server (www.baidims.org).***

A small shed housing two generators, a fuel depot, and 4000 feet of armored cable line initially powered the experiment and was placed half way between the road parking area and the manipulation site. This line was upgraded to a powerline from the city grid in 2007. For computer controlled activities near the experimental site, a small insulated and heated building called the "control shed" was installed. The control shed is wired to a 30-foot Rohn type tower adjacent to the building. The tower is host to multiple instrumentation including two common network domains, WAN and LAN that connect three eddy covariance towers on the manipulation site. The eddy covariance towers measure landscape-level carbon dioxide, water,

energy, and methane flux over the land-atmosphere boundary. A methane shed, smaller than the control shed, houses additional equipment that monitors methane flux. Tubing connected to instrumentation inside the shed extends out to wooden tripods out onto the manipulation site.

Tramline infrastructure that carries a robotic cart to perform ground-based hyperspectral remote sensing studies was placed adjacent to and south of the three boardwalks inside the manipulation area. The tramlines were extended 300 meters in 2006. Hydrologic engineers from Golder Associates designed a pumping system and three dikes to be placed inside the manipulation site. The dikes sectioned off each treatment area for the hydrologic manipulation. A v-notch weir was installed in 2007 as part of the dike in the control section to measure runoff. In 2004, a 100m grid was placed over the drained thaw lake basin used for snow surveys. A building called the "BEO Visitor Center" (not shown in Figure 3) was placed near the parking area off of Cake Eater Road in 2005. The building marks the beginning of the trail to the experimental site and can be utilized for science, education, and outreach activities.

2.2 Climate

The 29-year monthly mean climate data from NOAA (2006) is shown in Figure 4. Beginning in September and ending in May, the BEO has long, cold winters with a 29-year average winter temperature of -26°C in February and 122mm of snow (NOAA 2006). Cool summer conditions take place between June and August with a 29-year mean temperature of 3.3°C and 56.4mm of precipitation (NOAA 2006).

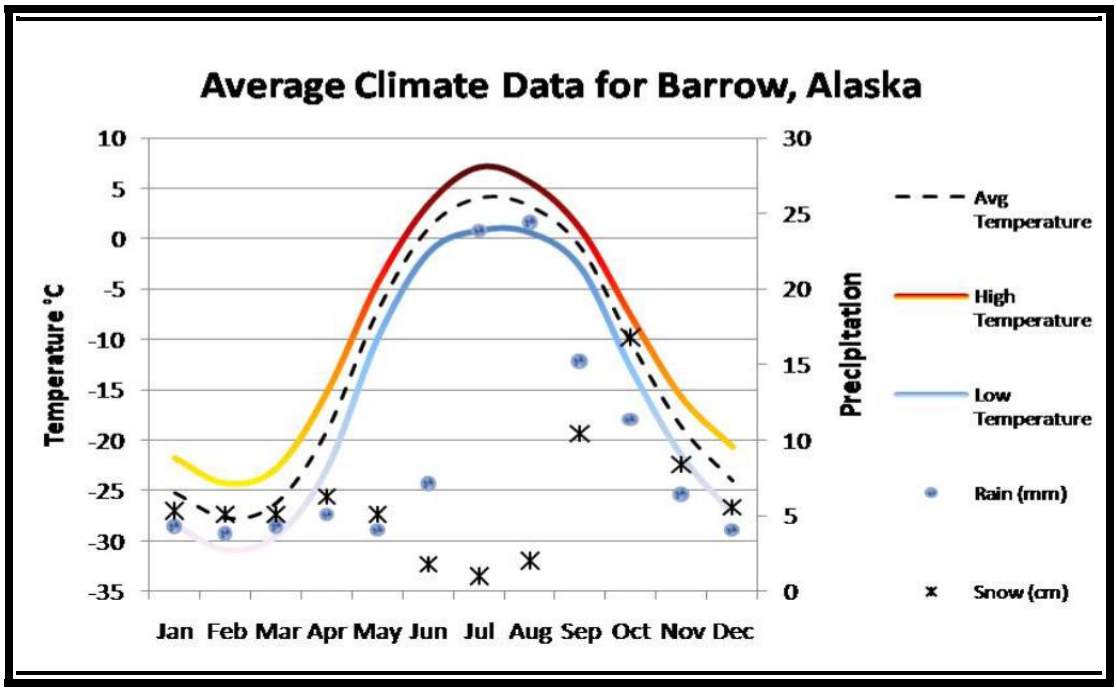

Figure 4. The 29-year mean climate data for Barrow, Alaska (NOAA, 2006). Barrow has very cold winters and cool summers. Precipitation is high during the summer months of July and August. Snowfall is greatest during October.

2.3 Physical Environment

The BEO has low relief with an average elevation of 4-meters above sea level (Aguirre *et al.* 2008). Seventy two percent of the coastal plain contains oriented lakes, drained thaw lake basins and small ponds (Hinkel *et al.* 2003). Geomorphic processes taking place within the study site include thermokarst terrain with low and high centered polygons, continuous permafrost to a depth of 400m, and a shallow 30cm active layer (Brown *et al.* 1980). The most prominent features of the study site, shown in Figure 5, are the relatively wet drained thaw-lake basin (dark area) surrounded by the drier and higher relief (light area) high-centered (a) and low-centered (b) polygonal tundra. An extensive description of the Barrow coastal plain can be found in a self-published book by Robert I. Lewellen (1972).

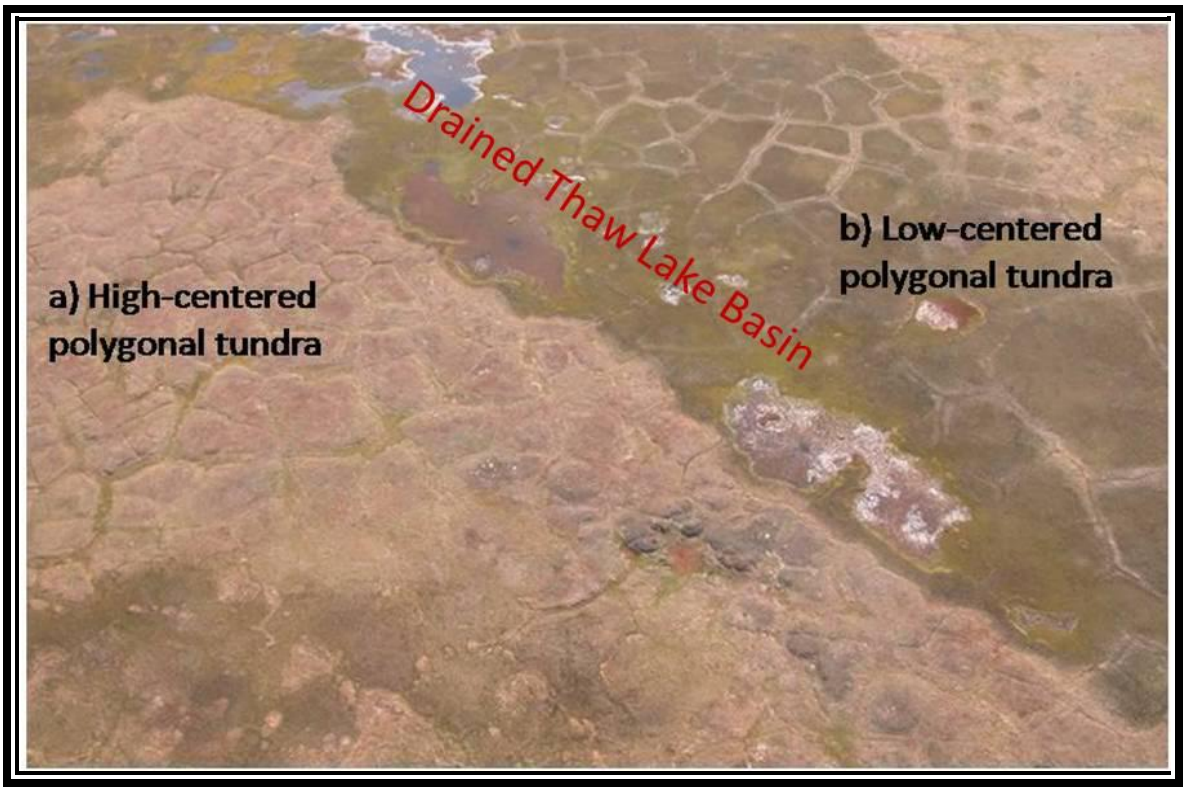

Figure 5. Prominent periglacial features at the Biocomplexity study site. The light area has higher relief than the dark (basin). High centered and low centered polygons are also labeled. ***Image courtesy of SEL, UTEP.***

Figure 6 is an Arctic Monitoring and Assessment Program (AMAP) illustration (Group 1988) that shows low centered polygons (a) with concave-shaped depressions able to capture water. Though not shown in the illustration, these depressions can turn into ponds, whereas high centered polygons (b) have a convex-shaped mound. The ice wedges shown can continue to grow and expand through the freeze-thaw cycle and create troughs and polygon rims in the process. Troughs can also function as water reservoirs (Hobbie 1980). Microtopographic features developed through these processes can exert great control over near surface soil moisture (Engstrom *et al.* 2005).

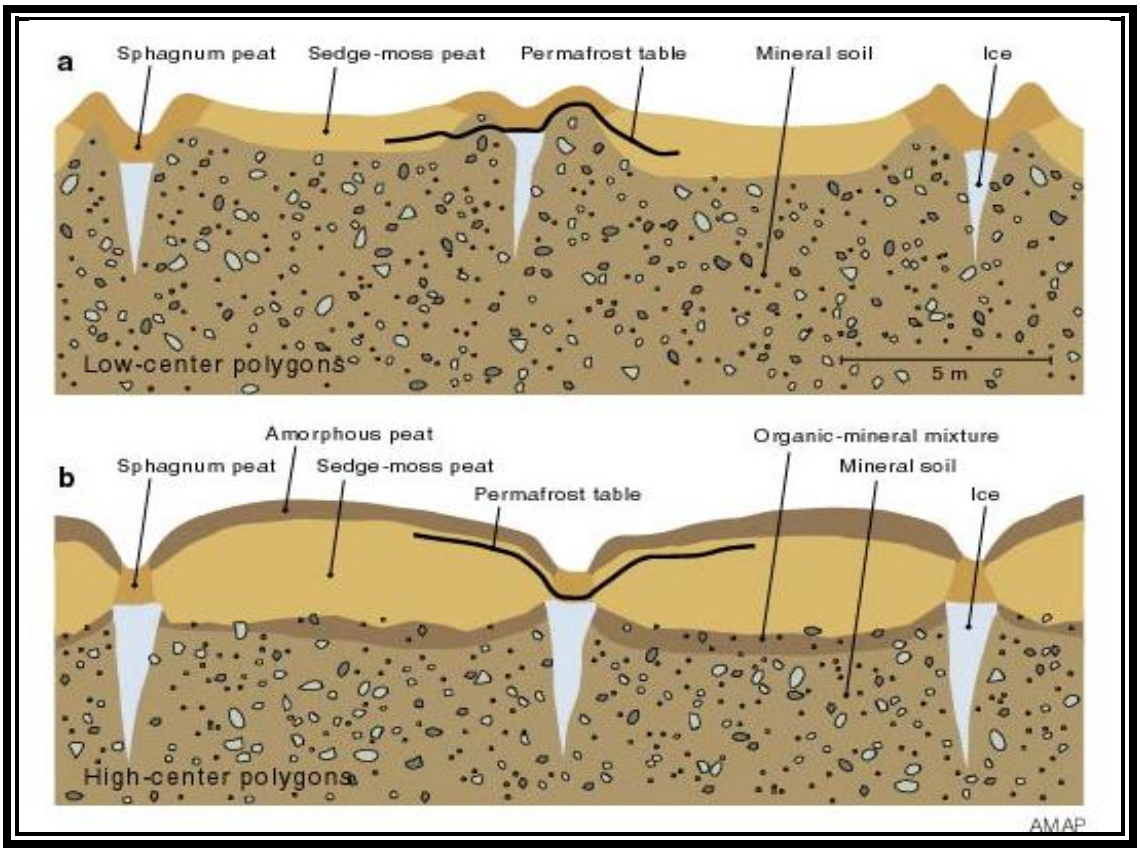

Figure 6. Illustration of low and high-centered polygons typical of those at the study site (a and b). The wedge-shaped depressions are ice-wedge troughs. Low-centered polygons (a) have concave-shaped depressions that may collect water. High-centered polygons (b) have convex-shaped mounds.

The dominant soils at the study site are Typic Cryosols, soils affected by frost action and permafrost (Tarnocai & Broll 2008). The upper 100cm of soil in Barrow is primarily carbon rich peat, estimated at 52kg/m3 (Bockheim 2007, Bockheim & Hinkel 2007). This is important because the high amount of carbon that is locked up in Arctic soils comprise approximately 25% of the global soil organic carbon pool (Bockheim & Hinkel 2007).

2.4 Biological Environment

Plant ecologists, who have studied arctic vegetation in Barrow through the International Biological Program (1964-1974), the International Tundra Experiment (1990's – present) and

other initiatives, typically describe land cover in the Barrow area relative to soil moisture status (Webber & Walker 1991, Hollister *et al.* 2006, Oberbauer *et al.* 2007). Figure 7 displays a satellite-derived land cover classification map showing vegetation distribution and a summary of the dominant vegetation cover. Ponded water at the study site makes up nearly 3% of the landscape. The most prominent landcover type is moist graminoid tundra with approximately 60% vegetation cover, and the most abundant graminoid is *Carex aquatilis*.

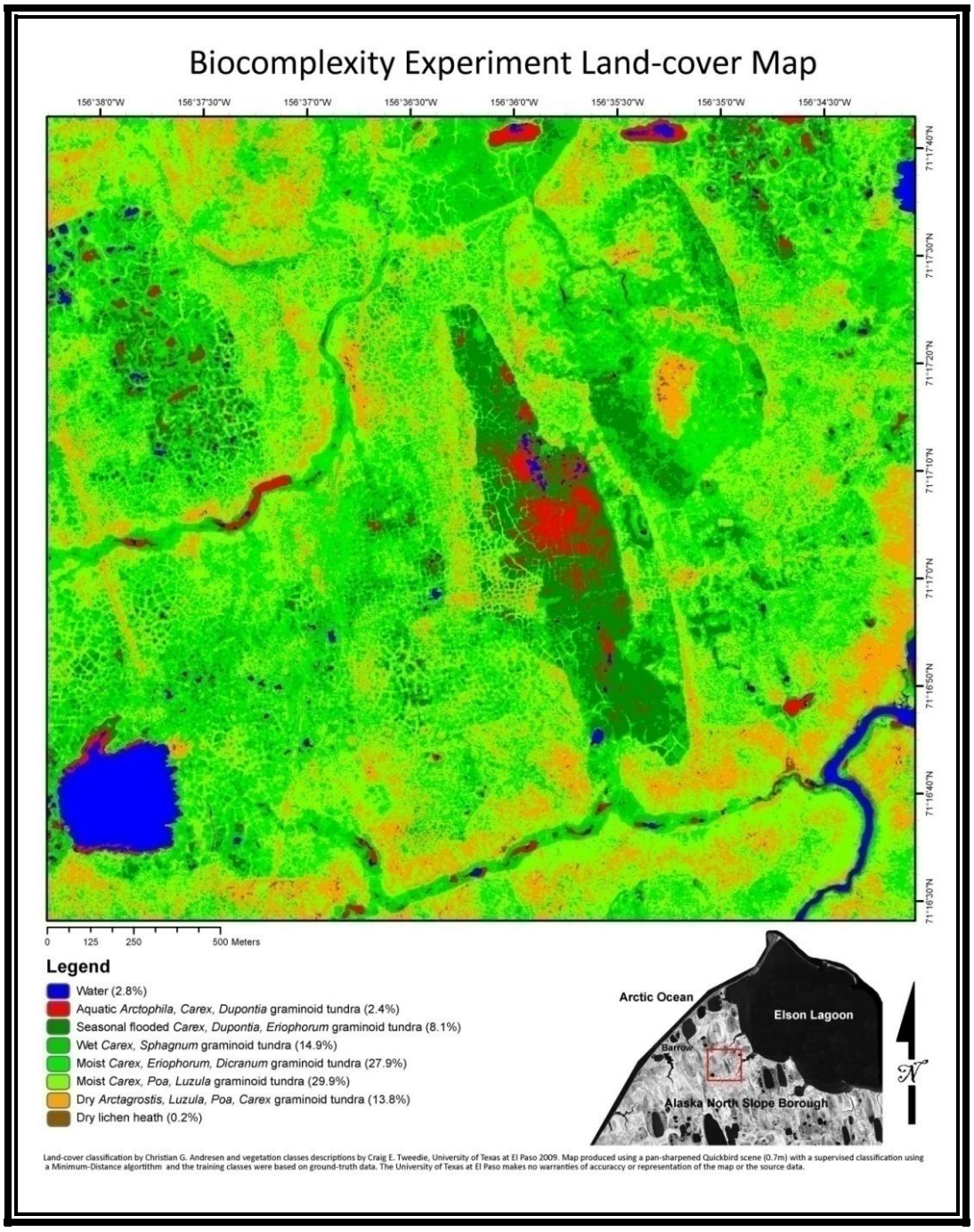

Figure 7. Land cover map of the study area. Land cover consists primarily of moist and wet graminoid vegetation (73%). ***Image courtesy of SEL Lab.***

Chapter 3: Methods

The following sections describe the methods used to gather data for this thesis. The analyses presented in this section were performed in Microsoft Excel 2007 and the statistical software JMP 8. Section 3.1 identifies the source of the climate data. Section 3.2 describes the methods used to attain LiDAR data in order to develop a digital elevation model (DEM) and characterize the DTLB watershed and its drainage patterns. Sections 3.3-3.6 describe the methods used to measure multiple hydrologic parameters including snow depth, active layer thaw depth, water table depth, and pond stage. Sections 3.4 and 3.5 highlight the statistical methods used to analyze water table depth and thaw depth prior to and during the hydrologic manipulation. In section 3.6, multiple 5^{th} order polynomial confidence curves fits are shown to observe patterns in pond water levels. Section 3.6.1 describes the Meyer evaporation equation (Subramanya 2008) used to calculate 2006 and 2007 summer evaporation rates. Pond temperatures were correlated to other climatic variables to test their relationship. All figures in sections 3.3-3.6 were created in Excel 2007, except for the confidence curve fits, created in JMP 8.

3.1 Climate Data

Monthly temperature, precipitation, wind, and solar radiation data from the NOAA Earth Systems Research Lab, (Global Monitoring Division's online U.S. Climate Reference Network) were attained to plot summer climatic conditions at the study site for June-August of years 2005 through 2008. The station used for data collection is NOAA's Barrow Observatory (BRW-ENE), in close proximity to the study site. Temperature and precipitation were compared to the

29 year mean from NOAA's National Weather Service Online Data (NOWData), using the summer months June, July, and August.

3.2 LiDAR Used for Watershed Delineation

LiDAR is the acronym for Light Detection and Ranging and is a remote sensing tool that uses ground or airborne sensors with a pulsating laser to intercept ground objects (Donnellan *et al.* 2008). In airborne LiDAR, a global positioning system unit can be attached to a plane to produce 3D-geographical location points with elevation as shown in Figure 8 (Luo & Gavrilova 2006). LiDAR has been effectively used in multiple ecological studies ranging from habitat and vegetation mapping and classification (Lefsky *et al.* 2002, Streutker & Glenn 2006, Bork & Su 2007, Lee & Lucas 2007) to bird species characterization (Clawges *et al.* 2008). A more detailed explanation of what LiDAR data acquisition entails and the application of this remote sensing tool in ecological studies can be found in Vierling et al. (2008).

In this study, the OPTECH ALTM 70 kHz LiDAR system was mounted on a twin-engine Cessna 310 aircraft in October 4, 2005. LiDAR data was acquired at 600m from the ground with a horizontal accuracy of 30cm, a vertical accuracy of 15cm or better, and a point spacing of approximately 0.6m (information based on provider metadata). The dataset was post-processed by the provider, using three software packages: REALM, TerraSolid's "TMatch", and "TerraScan" to classify data into "1st pass" and "last pass". Data having points that first intercepted an object was classified as "1st pass". "Last pass" data points were reclassified as "bare earth," since these points traveled farthest and intercepted objects with the lowest elevation – assumed to be the ground surface. The dataset was output to a comma delimited "Point Cloud" ASCII text format.

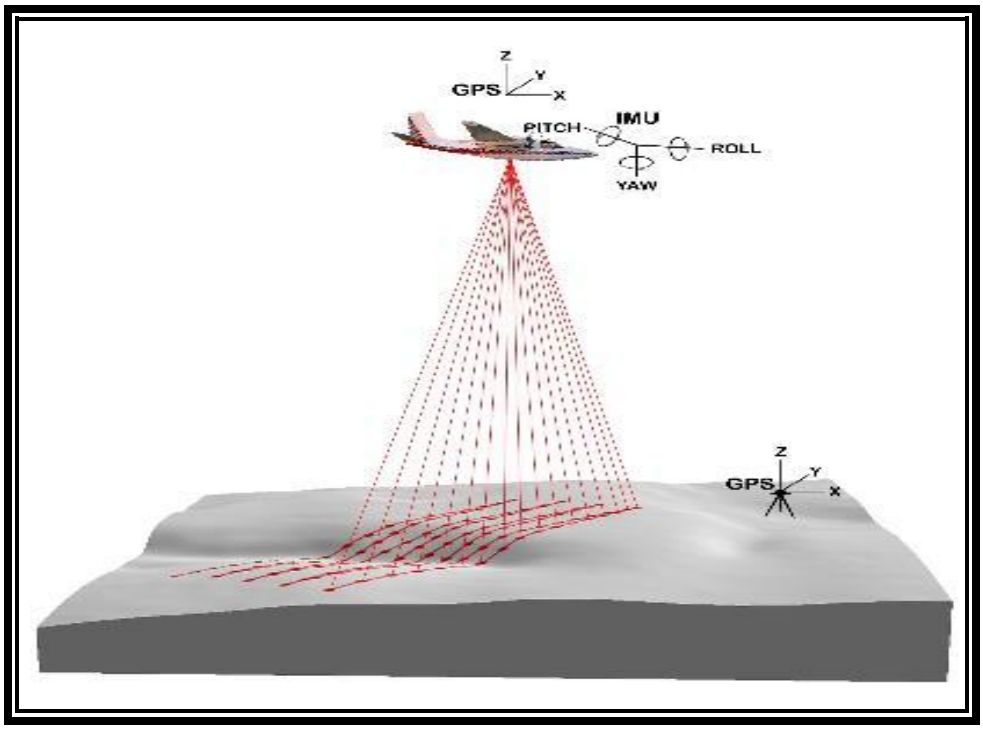

Figure 8. Airborne LiDAR image. Shown is a two engine plane sending laser pulses to the ground with an altimeter sensor and GPS to produce 3D geographical coordinates. Image courtesy of the PNW Research Station, Washington State University (http://forsys.cfr.washington.edu/JFSP06/lidar_technology.htm)

To begin the rasterization process, the text files were input into ESRI's ArcGIS 9.2 Geographic Information System (GIS) software and converted to shapefiles. The 3D Analyst application was used to build tin files out of the shapefile point cloud and then convert the tin files into a raster layer with 1m pixels. DEM accuracy was checked using tundra pond elevations from ponds 5, 6, 7, and 12. They were cross-referenced to tundra pond elevations measured with DGPS at peak water levels, and the elevations matched. This study also utilized the method of Streutker and Glenn (2006) to check LiDAR accuracy, and analyzed a collection of points from a flat surface – such as a body of water, to find the standard deviation and subsequent variability within the LiDAR dataset. In this study, a rectangular area from Pond 1, which included 30,393 points from the bare earth dataset, was used to test for LiDAR errors using this method. The DEM was compared to a Quickbird Satellite image to observe how much detail was captured in the DEM that might have been missed in the satellite image. The

Quickbird Imagery was acquired August 2, 2002 by DigitalGlobe (Tweedie & Gaylord 2006). This satellite image has a 0.7m resolution and is an excellent resource for analyzing land surfaces in detail. A slope DEM was also created in ArcGIS to observe prominent features on the tundra and verify that the ponds were not troughs. Using the spatial analyst extension of ArcGIS, the slope function was selected to analyze each cell and produce a DEM expressed as the greatest rate of change between each neighboring cell.

ArcHydro was chosen to model the basin's watershed because it is designed to work explicitly with ArcGIS and is a data model for water resources (Maidement 2002). The ArcHydro "Terrain Processing" tool was used in the order that the instruction manual indicated (ESRI 2007). First, the DEM's grid was reconditioned and smoothed out for further processing. Thousands of sinks were filled with the "sink" command, which may have included hundreds of low-centered polygons in the form of ponds that Macrae et al. (2004) describe as individual microcatchments in northern peatlands. A "flow accumulation" and "flow direction" command used the elevations from nine contiguous grids, by looking at the center grid and assessing which of the other eight grids a drop of water will run to. The flow direction was then used to produce a stream network. A somewhat dense network was selected by inputting "4000" cells equivalent to 0.025km into the "Stream" layer. After the stream network was created, the catchments of the area were processed. Following the creation of the catchment DEM, batchpoints were inserted in different areas of the DEM so that drainage lines and basins could be delineated.

LiDAR and raster data processing was a challenging task, due to the approximately 12 million points in the LiDAR dataset. As Arge et al. (2003) state, processing large datasets in different terrain software can cause software to slowdown or fail because the software's algorithms are aimed at computer efficiency and not at maximizing computational needs. Furthermore, processing time for datasets is dependent on topography because a small dataset with flat terrain takes longer to process than a large mountainous - high relief dataset (Arge *et al.* 2003). In order to avoid software failure in ArcHydro, the amount of data being processed was reduced by resizing (clipping) the DEM and focusing on the immediate area surrounding the

DTLB. Nonetheless, a smaller, yet high-resolution (1m) DEM was integrated into ArcHydro to define the DTLB drainage lines and catchments.

3.3 Snow Depth and Snow Water Equivalence (SWE)

In late April 2006, snow depth was measured on the 100m grid laid across the DTLB that contained 130 marker points (Figure 9). Similar snow depth and coring methods to Sturm and Liston (2003) were used. First, a 1m graduated metal rod was thrust vertically through the snowpack until it hit frozen ground and depth was recorded. To measure snow depth, three different measurements were taken at each marker. For the first 34 markers, a half-meter long ABS pipe with a 5.74 cm diameter was hammered into the snow until it hit frozen ground. Snow inside the pipe was collected by sliding a plastic bag under the pipe to catch the snow when the pipe was lifted. Snow depth was also recorded on the side of the pipe. The bags with the snow were taken back to the lab and the snow was left to melt. Once the snow melted, the volumetric content was measured to obtain snow density (g/cm^3). Snow water equivalence (SWE) was calculated by dividing snow depth by snow density and scaling the measurement to kg/m^2. This number was then converted to water in mm. Snow depth and snow (for SWE) were also collected for spring 2007 and 2008, however, due to logistical constraints, these measurements were carried out in late May. The 300m boardwalks were used as transects in 2007, where snow was measured at 10 meter intervals. In 2008, the 100m grid was used to collect and measure snow depth and SWE data. Snow sublimation or ablation can be difficult to account for (Sturm *et al.* 2001) and was not measured.

3.4 Water Table Depth

Water table depth (WTD) was measured on the south side of each 300m boardwalk and immediately adjacent to the tramline footprint inside the experimental area (Figure 9). White PVC pipes were drilled into the ground at every 30 meters along each of the 300m boardwalks. Measurements were made every few days during the summer snow-free period between

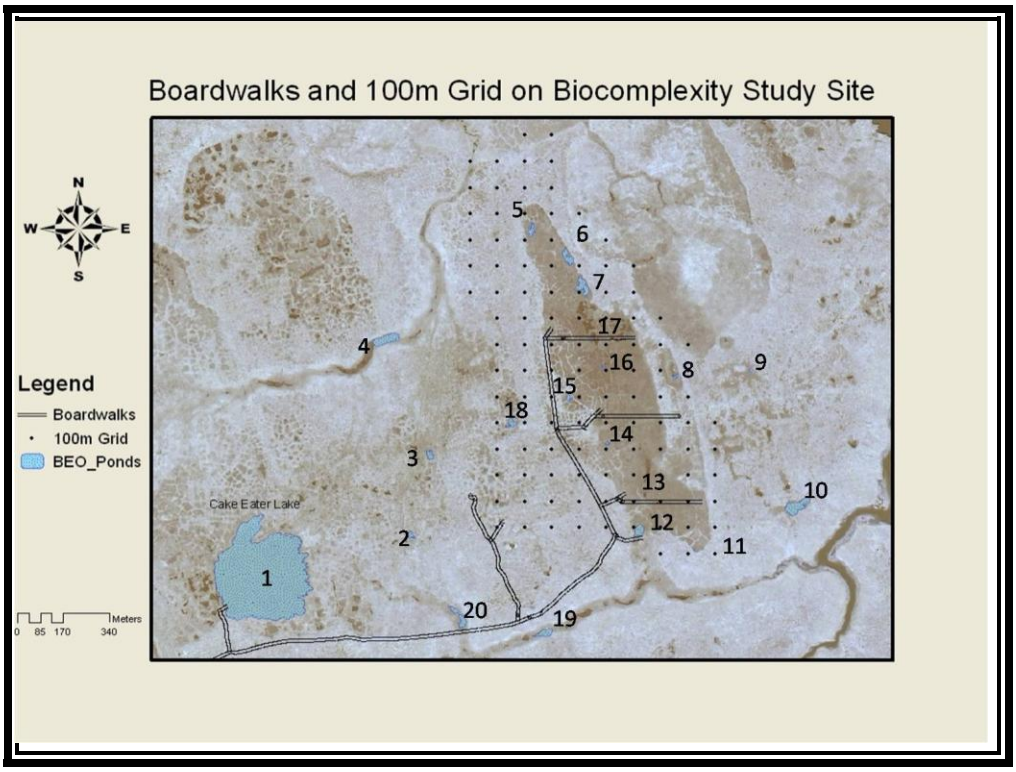

Figure 9. Map of 100m grid. Study site showing a 100m grid represented with black dots, used for snow depth measurements. The brown lines are the boardwalks. The straight lines in the middle of the figure are the 300m boardwalk used to study the control, drained, and flooded treatment areas of the DTLB. The experimental ponds are represented with their respective number.

mid June and mid August of 2007 and 2008. WTD was calculated by subtracting the distance between the top of the pipe to the water table from the distance between the top of the pipe and ground level. DGPS measurements were taken of the top of the water table markers periodically throughout the summer to correct height to an absolute measure. Measurements were not taken where there was snow cover during June, and where there was interference or disturbance from

other experimental structures, or if WTD tubes were dry at the upper surface of permafrost (a common occurrence in 2007). Water table depth measurements for summer 2007 were averaged per day and treatment, totaling 14 days of measurements for each treatment: control, drained, and flooded. The same was done for 2008. In order to compare the difference between treatment and non-treatment years, the drained and flooded WTD values were subtracted from the control for 2007 (pre-treatment) and 2008 (treatment year) respectively. A Shapiro-Wilk test was performed on the 2007 and 2008 mean datasets to confirm that they were normally distributed. Finally, a two-paired sample t-test was used to observe pre and post treatment effects for 2007 and 2008.

3.5 Thaw Depth

Thaw depth was measured along each of the three DTLB boardwalks (Figure 9). The boardwalks were treated as linear transects and thaw was measured by thrusting a metal rod into the ground until a solid bottom was hit. Thaw depth was recorded at every meter along the south facing side of the boardwalks every 2-3 weeks in summer of 2007 and 2008. Measurements began at the western end of each boardwalk and ended at the eastern end. All data were collected using the Circumpolar Active Layer Monitoring program's (CALM) mechanical probing protocol (Nelson *et al.* 2007). In order to compare differences between years and treatments, the drained and flooded thaw depth values were subtracted from the control, assuming that the differences for each year would be zero if a treatment effect was not observed. A Shapiro-Wilk test was performed on the 2007 and 2008 datasets to test for normality. The data was not normally distributed, therefore a Wilcoxon matched pairs signed rank test was performed to observe pre and post treatment effects for 2007 and 2008, respectively.

3.6 Pond Water Level Measurements

The experimental ponds at the study site consisted of one lake, three ponds in ephemeral-streams, and 16 ponds associated with low-centered polygons (see Figure 9). The area (derived by digitizing the pond surface from 2002 QuickBird Satellite imagery), elevation, location, type, and experimental area of each pond is shown in Table 1. Elevation, in Table 1, was derived from pond water level measurements taken in early spring because that is when water levels are highest. Ponds were chosen according to their proximity to the Biocomplexity experimental area. Ponds outside of the DTLB were used as controls for the control ponds inside the manipulation area. Ponds inside the manipulation area were situated among the three treatment areas (flooded, drained, control), and were used to the effect of experimental manipulation of soil water.

Table 1. List of ponds at the Biocomplexity study site.

Pond No.	Area (m_2)	Elevation (m)	Latitude	Longitude	Pond Type & Experimental Treatment
1	98993	4.37	71.2780304	-156.628885	Lake - control
2	532	4.03	71.27972813	156.6188967	Polygon - control
3	206	4.14	71.28229752	156.6162427	Polygon - control
4	3804	3.49	71.28645856	156.6197291	Stream -control
5	895	4.1	71.29009043	156.6050004	Polygon – exp flooded
6	1240	4.04	71.28895768	156.6012823	Polygon – exp flooded
7	1966	3.99	71.28814285	156.5999002	Polygon – exp flooded
8	256	4.03	71.28481893	156.5907406	Polygon - control
9	118	3.92	71.28491841	156.5832739	Polygon - control
10	3064	3.53	71.28002614	156.5790727	Polygon - control
11	23	4.09	71.27888781	156.5897636	Polygon - control
12	1302	3.66	71.27949608	156.5957362	Polygon – exp control
13	8	4.07	71.28057639	-156.595578	Polygon - control
14	31.2	4.12	71.28257427	156.5985587	Polygon –exp control
15	397	4.17	71.28427801	156.6018245	Polygon – exp drained
16	125	4.06	71.28524674	156.5983643	Polygon – exp drained
17	74	4.08	71.28623957	156.5997566	Polygon – exp drained
18	772	4.06	71.28345947	156.6075349	Polygon - control
19	1320	2.66	71.27649129	156.6138253	Stream - control
20	1759	3.12	71.27631023	156.6047479	Stream - control

Figure 10 shows the 20 pond locations (10 within the experimental area and 10 outside of the experimental area). The ponds were marked in the following manner: 1 meter-long sections of rebar were pounded into underlying permafrost using a Hilty Drill. Black ABS pipes, measuring 1.5m x 3.81 cm diameter, were placed over the rebar and left as a permanent location marker for our monitoring sites. An antenna mount for a Differential Global Positioning System (DGPS) was crafted out of a 5cm diameter ABS pipe so that it fit snuggly over the permanent markers.

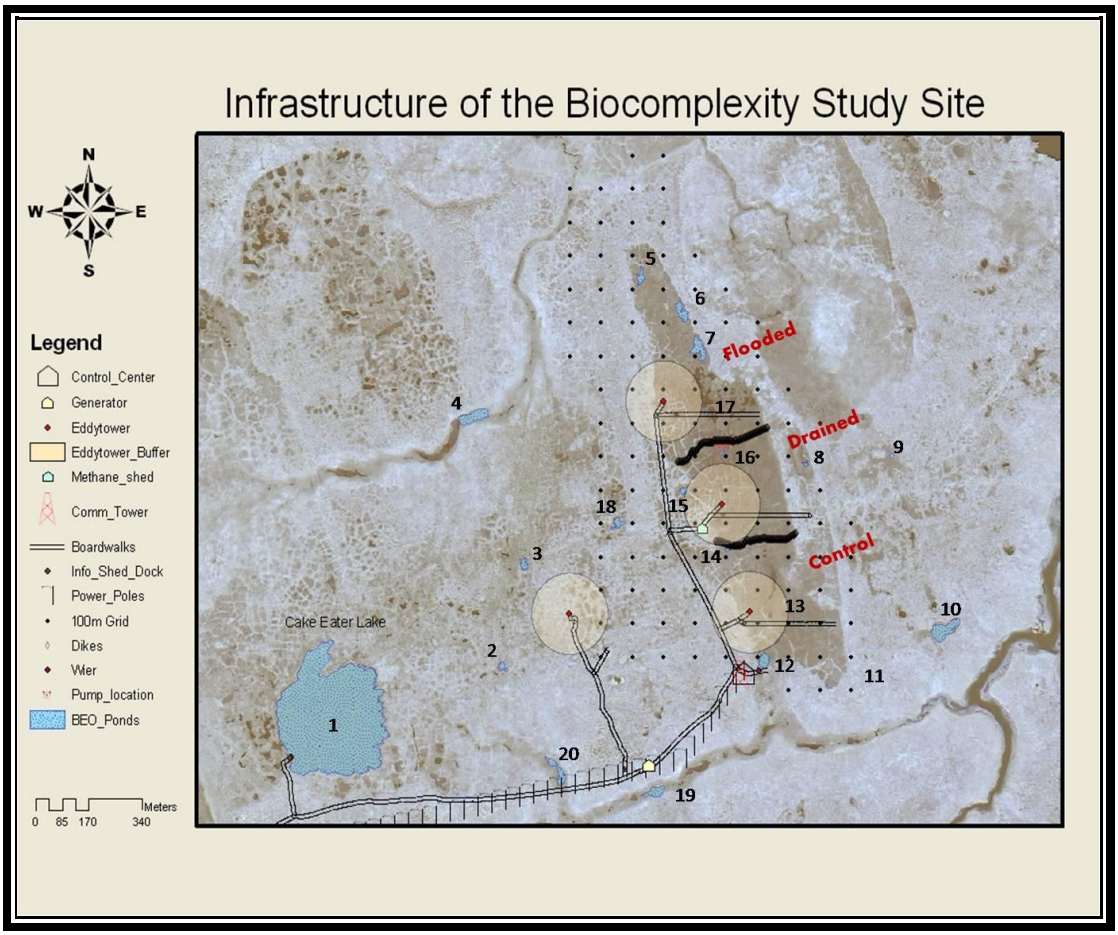

Figure 10. BEO Ponds monitored for the Biocomplexity Experiment. Twenty ponds (shaded light blue and numbered) are shown, along with the boardwalks and tramlines. The black lines are the dikes that separate the flooded, drained, and control treatment areas labeled in red.

Remote GPS field data collection was made using DGPS technologies. A TrimbleNetRS GPS receiver with a Zephyr Geodetic antenna mounted on top of the BASC building served as the base station. The rover system used to track water level changes in 2005-2006 was a Trimble 5700 receiver with a Zephyr antenna and a Trimble TSC1 controller. In 2007, a new rover system was used: Trimble R7 with an internal radio and a TSC2 survey controller to log field data. A Trimble HPB450 radio provided real time kinematic survey capacities to the rover DPGS unit most of the time. All DGPS equipment was provided by UNAVCO (www.unavco.org) for all field seasons.

Every summer season from 2005-2008, except for 2007, field assistants surveyed each of the 20 ponds, one to several times per week, by positioning the Zephyr antenna on the pond marker. Due to logistical constrains, water levels were not available for mid July to September in 2006. Depending on good or bad radio signal, one of two survey methods or both were used to collect data using the rover GPS: Real time Kinematic (RTK) when there was radio signal and Post-Processed Kinematic (PPK) or a static survey when there was no radio signal. RTK surveys require a radio link to the base station whereas PPK and static surveys do not require a radio link, but do require differential correction between data logged in the field and data logged at the base station for centimeter-accuracy. The post processing is described immediately below.

Rover DGPS data were downloaded into the Trimble Geomatic Office Software version 1.63 (TGO) to correct data collected using PPK or static survey methods and/or export corrected data to a text file. Once the text files were opened in Excel 2007, the difference between the base of the Zephyr antenna and the pond water surface was removed from the DGPS ellipsoid height to attain an absolute pond surface water level (Figure 11). Water levels were monitored every 3-5 day intervals in 2005-2006. The monitoring interval increased to every other day and daily in 2007 and 2008, respectively. Pond levels for all ponds were plotted in Excel 2007 for each year. A 2-day moving average was calculated to assess water loss from the ponds. In JMP 8, a bivariate fit (water level by time) was chosen to get a 95% confidence curve fit for all ponds in their respective year and assess any patterns in the water level fluctuations.

In order to observe possible treatment effects on pond water levels, the pond water levels were totaled at the end of the season and were separated into their respective treatment areas. Those totals were averaged out by treatment section. Using JMP 8, a Shapiro-Wilk test was performed on the averages to test for normality. The data was not normally distributed, therefore

a Wilcoxon matched pairs signed rank test was performed to compare each treatment section by year and observe possible pre and post treatment effects for 2005, 2006, 2007, and 2008.

In 2007, an attempt was made to begin the manipulation by pumping water into and out of the proposed sections, but the pumping system failed in early June, so only the ponds with the level loggers and the ponds inside the DTLB were monitored. In June 2008, the pumping system was put in place once again and pumping was sustained for the entire snow free season. During 2008 the ponds were monitored every day so that water levels in each treatment section could be adjusted to their respective treatment, using the pumping system to stay at the ±10cm target.

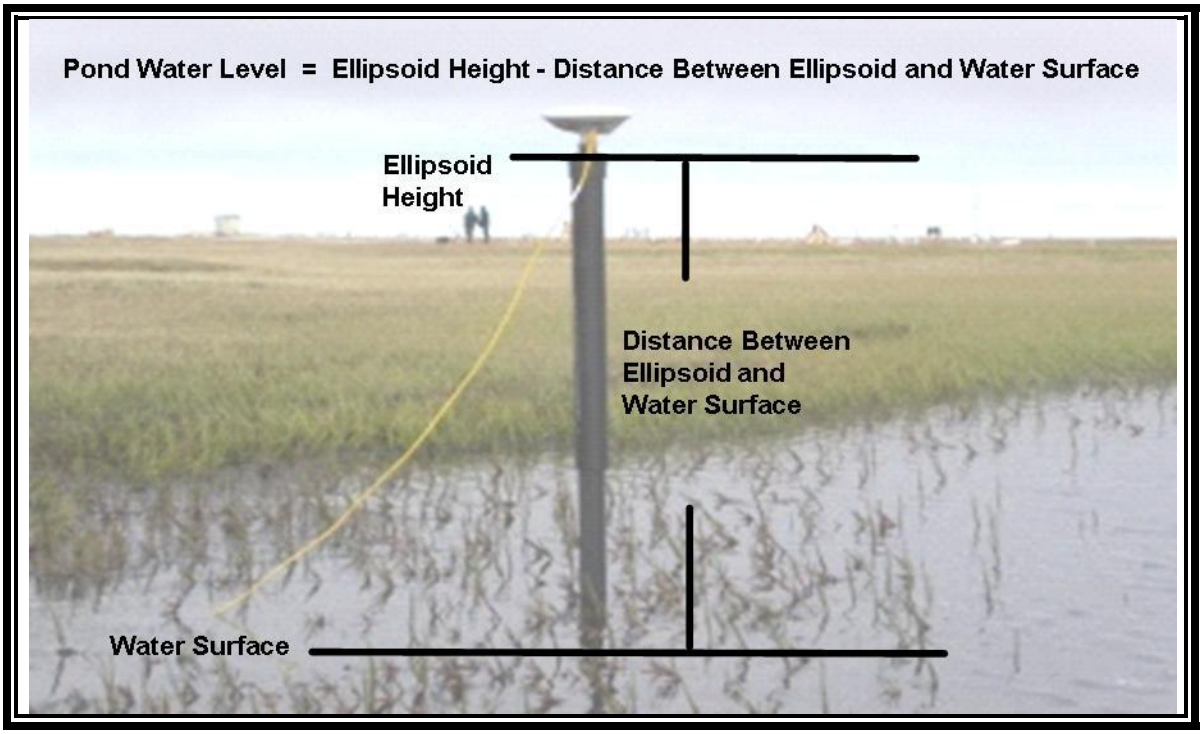

Figure 11. Photograph of pond water level measurements using DGPS. The distance between the ellipsoid height and the pond surface was removed to get an absolute water level (cm).

Pond pressures and temperatures were monitored in 4 ponds during the summers of 2006-2007 with HOBO U20 Water Level Loggers (Figure 12). The level loggers were set up to measure pressure in *psi* and water temperature in degrees Celsius. Data was downloaded from

the level logger and exported to Excel spreadsheets. Pond pressure was averaged out to daily values and corrected for atmospheric pressure. Pressure is presented in kPA and plotted with precipitation to note patterns. Pond temperature was recorded at 10 minute intervals and averaged to daily values. The pond temperature data was averaged out by month to help calculate evaporation. Water pond temperature was regressed against air temperature and total solar radiation to assess any positive relationship.

Figure 12. HOBO H_2O Water Level Logger

3.7 Evaporation

Evaporation was calculated by using Meyer's formula (Subramanya 2008):

$E = C(e_s - e_a)^* [1 + W/16]$

- E = evaporation (mm/day).
- **C** is a coefficient for daily data: approximately 0.5 for small shallow ponds and 0.36 for large lakes and reservoirs. The arctic ponds studied in Barrow are small and shallow, thus 0.5 was used.
- **e_s** is the saturated vapor pressure in mmHg at the water surface corresponding to the water temperature
- **e_a** is the actual atmospheric vapor pressure in mmHg, from the saturated vapor pressure (from the given air temperature in ºC) multiplied by relative humidity. Relative humidity data was compiled from the San Diego State University Global Change Research Group (http://gcrg.sdsu.edu/)

- **W** is average monthly wind speed in km/hr. This data was compiled from the San Diego State University Global Change Research Group (http://gcrg.sdsu.edu/)

Temperature data is from NOAA's Barrow Observatory (BRW-ENE), in close proximity to the study site. Water pond temperature is from the data loggers.

Chapter 4: Results

Results for climatic conditions at the study site for the years 2005 through 2008 are presented in section 4.1. Results from LiDar-derived data are explained in sections 4.2. Section 4.3 presents results for snow depth and SWE. Section 4.4 presents water table depth (WTD) and Section 4.5 presents results for thaw depth, with their respective statistical analysis. Section 4.6 presents pond water level plots from data. Pre and post analysis of pond water levels are also included. Pond water temperature plots are presented in section 4.7 and evaporation estimations for 2006 and 2007 are shown in section 4.8.

4.1 Climatic Conditions 2005-2008

Climatic data for the 2005-2008 field seasons is presented in Table 2 against the 29-year mean for Barrow, AK. All years were cooler than the 29-year average, except for 2007, which was 1.3'C warmer. Precipitation was variable, yet the average of 2005, 2006, and 2008 was 5.2mm higher than the 29-year average and 2007 was 43.5mm lower.

Table 2. Climate Data Summary. The table includes mean precipitation and temperature recorded by NOAA (2006) for 29 years and mean precipitation and temperature for the cumulative months of June-August.

YEAR	PRECIPITATION	TEMPERATURE
1971-2000	56.4mm	3.3°C
2005-2008	49.4mm	3.1°C
2005	68.6mm	2.7°C
2006	72.4mm	2.6°C
2007	12.9mm	4.6°C
2008	43.7mm	2.6°C

A time-series plot is presented in Figure 13 for June, July, and August of 2005-2008 with mean summer temperature being 3.1 °C. Summer 2007 had the highest mean summer temperature at 4.6 °C. Total summer precipitation at the study site for summers 2005-2008

averaged 49.4 mm, with 2007 showing only 12.9 mm of rain. The summer of 2007 was particularly hot and dry compared to 2005, 2006, and 2008. Trend lines marked with dashed lines across the plot show a warming and drying trend for the study period.

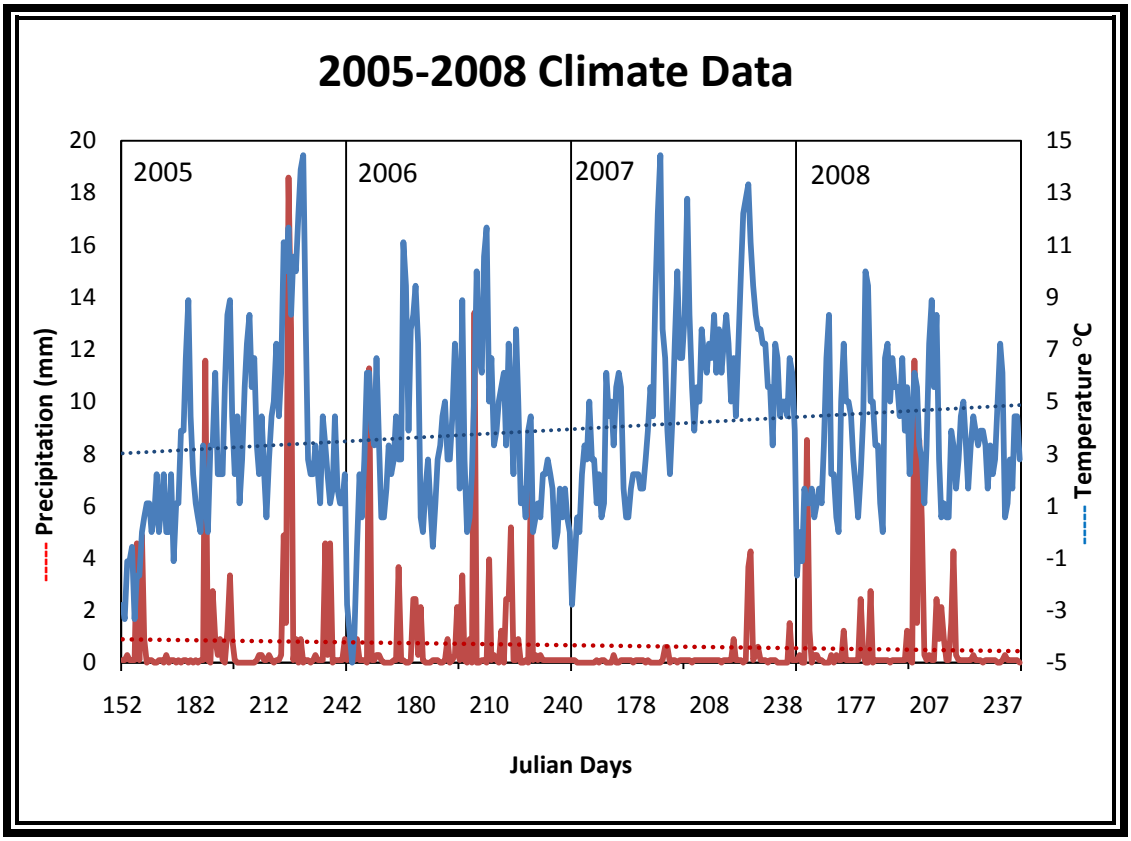

Figure 13. Temperature and precipitation for Summers of 2005-2008 in Barrow, Alaska (NOAA, 2010). Trend lines show slight heating and drying during the summer field seasons.

4.2 LiDAR-Derived DEM

A clipped 1-m-resolution DEM was produced from the LiDAR "bare-earth" dataset (Figure 14). The highest elevation shown on the figure is 5.2m and the lowest elevation is 3m, shown in grey. The average elevation was 4.09m with a standard deviation of ±0.42m. Using the Bare Earth grid, +30,000 points were analyzed from Pond 1 to test for LiDAR errors yielded

an average elevation of 4.66m with a standard deviaton of 0.1m. The maximum elevation was 4.94m and the minimum elevation was 4.22m.

Some of the more prominent features captured in the DEM are the many tundra low and high centered polygons surrounding the manipulation area. In Figure 15, a Quickbird Satellite image is compared to the LiDAR DEM. Red arrows point to some large polygons as reference. Images (a) and (b) both show tundra polygons surrounding the flat part of the experimental basin. Note the areas inside the red rectangle in images (c) and (d). The vegetation in (c) does not allow for the polygons to show up in the satellite image, whereas the LiDAR image (d), which can penetrate vegetation, captures the patterned ground with fine detail.

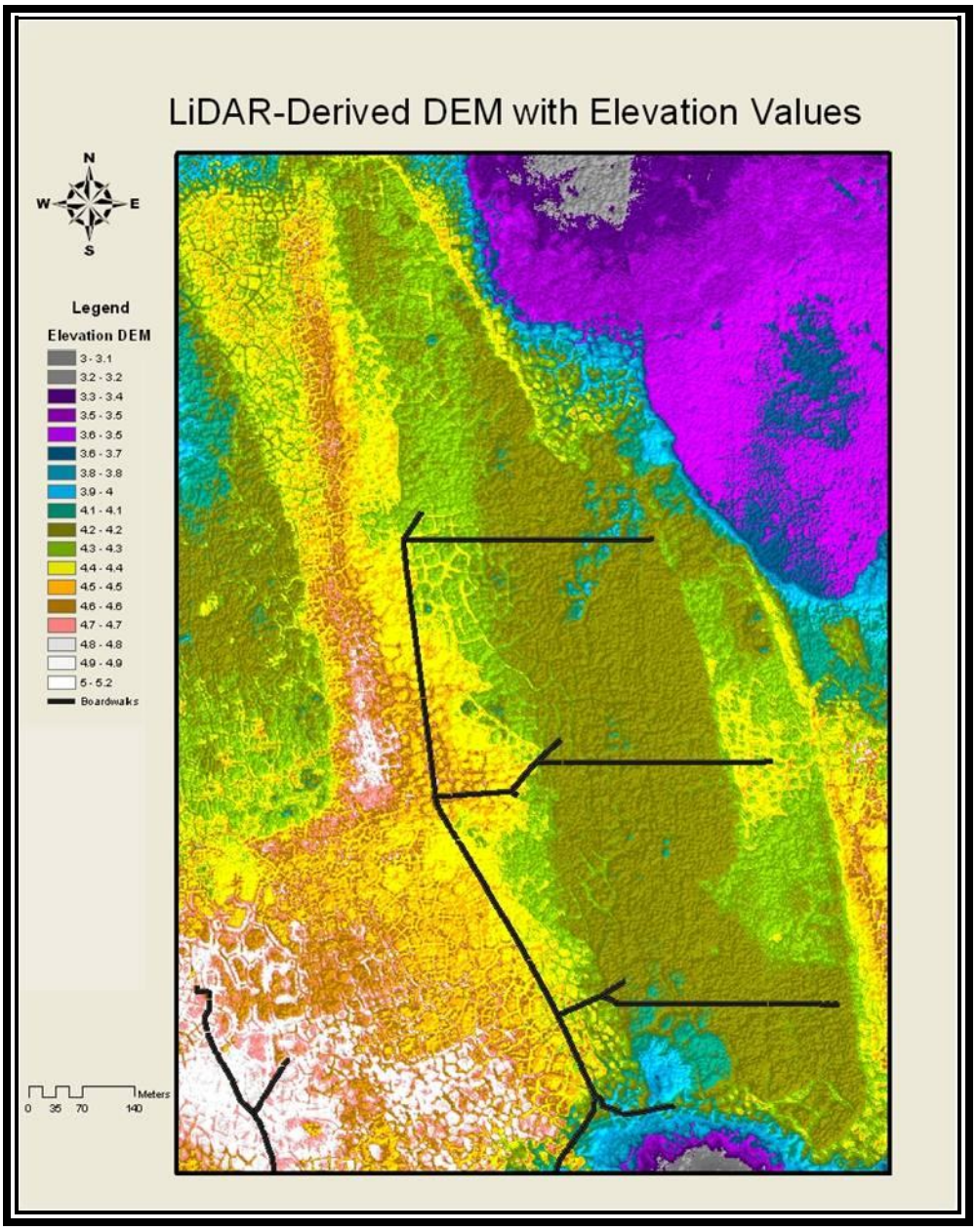

Figure 14. LiDAR-derived DEM with color-coded elevations. The boardwalks shown in black were added as reference to color-code the areas perceived to be part of the manipulation site. The flat part of the manipulation area is colored brown, encircled with a green and yellow rim.

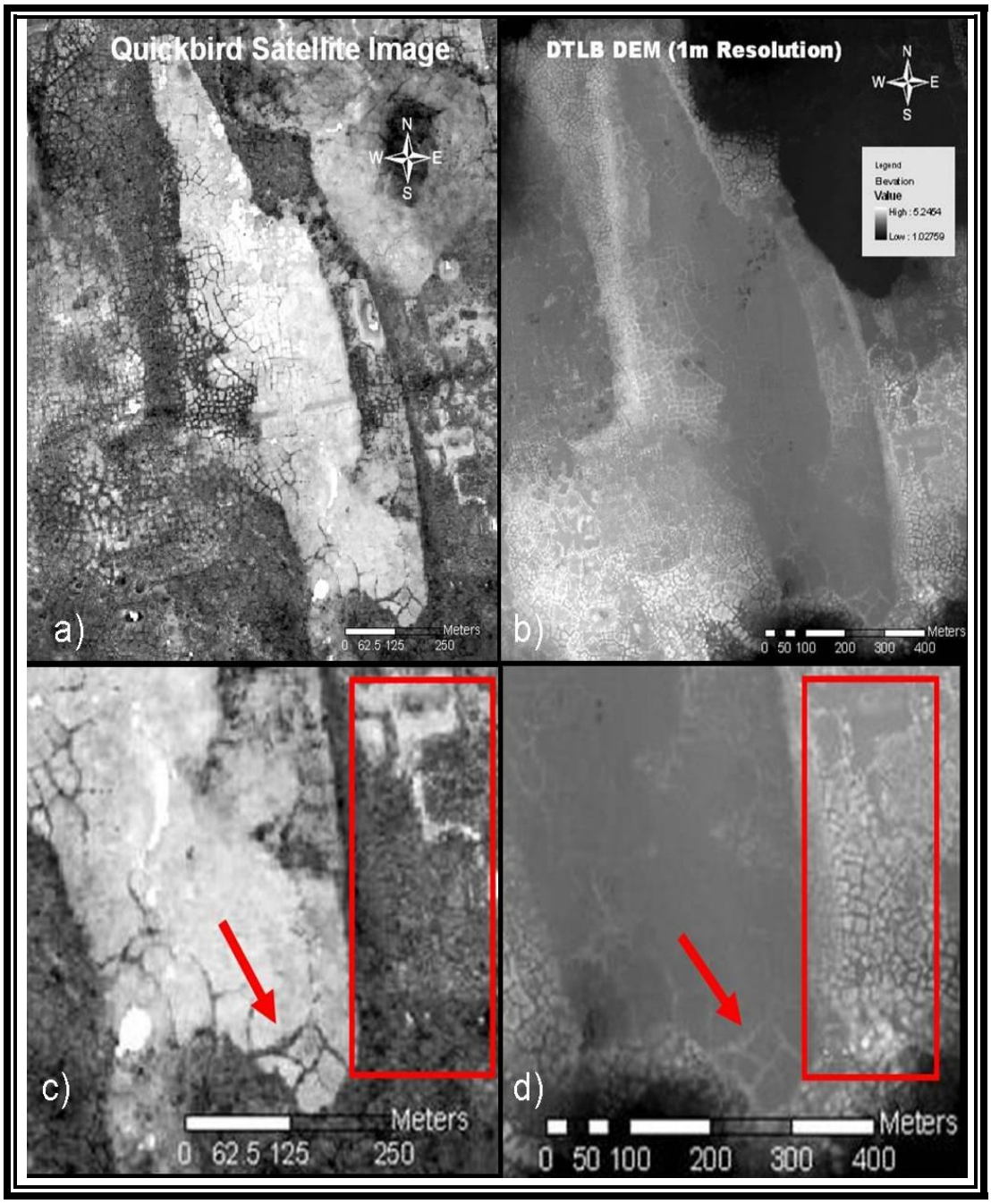

Figure 15. Comparison between the Quickbird Satellite Image (a) and LiDAR derived DEM (b). Note the fine details of polygonized tundra that were captured in the red box of the zoomed DEM image (d), which are not visible in the satellite image (c). The red arrows point to four tundra polygons used as reference when zooming in to each image.

A slope DEM (Figure 16) of the study site was created with units showing slope percent. Overall, the area has an average slope of 2.97 % (*ca*. 2 degrees), with a standard deviation of ±2.7 %. The highest slope percent was 43 and the lowest slope value was zero.

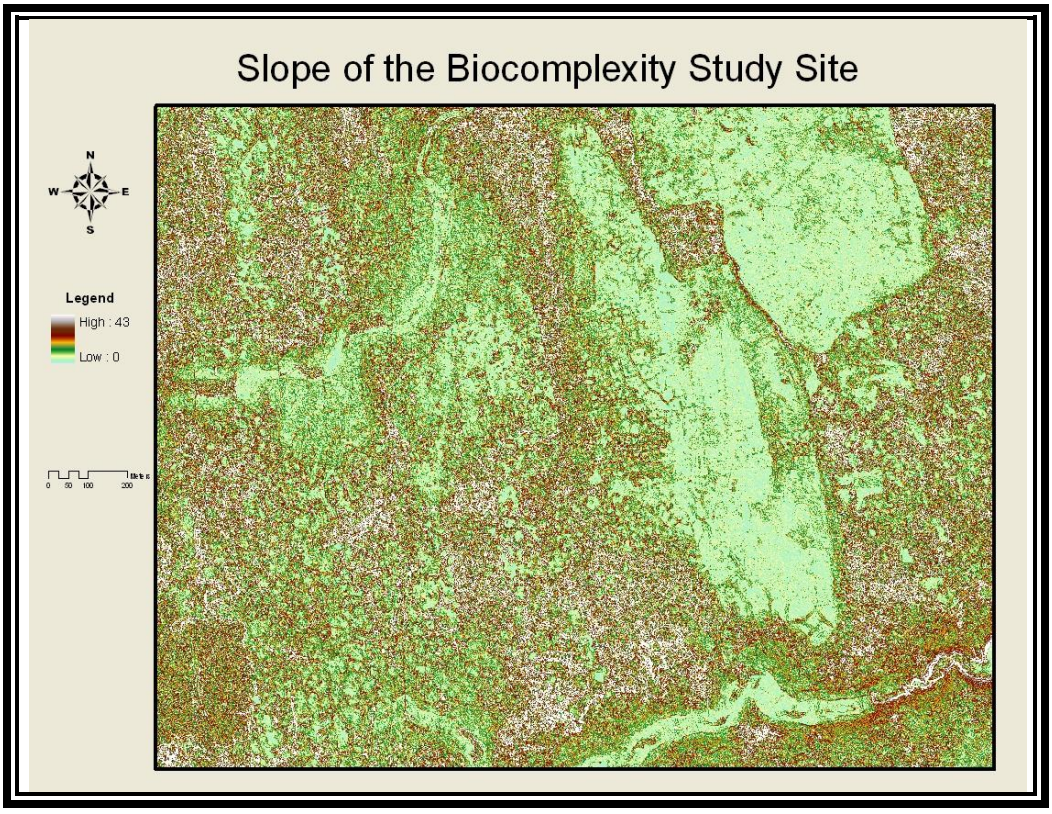

Figure 16. Slope DEM of the Biocomplexity Study Area. Note the green patches on the right hand side of the image with a slope percent close to zero, indicating that these regions are very flat basins.

The experimental basin produced from ArcHydro defined two catchments within the manipulation area and two outlets (Figure 17). The northern catchment was 389,167m^2 in area, whereas the southern catchment had an area of 219, 400m^2. The model produced two outlets, one on the northeastern part of the basin, and the other at the southern part. The NE outlet was dammed in 2008 to make sure that no water was escaping the basin and only the southern outlet was used for flow measurements.

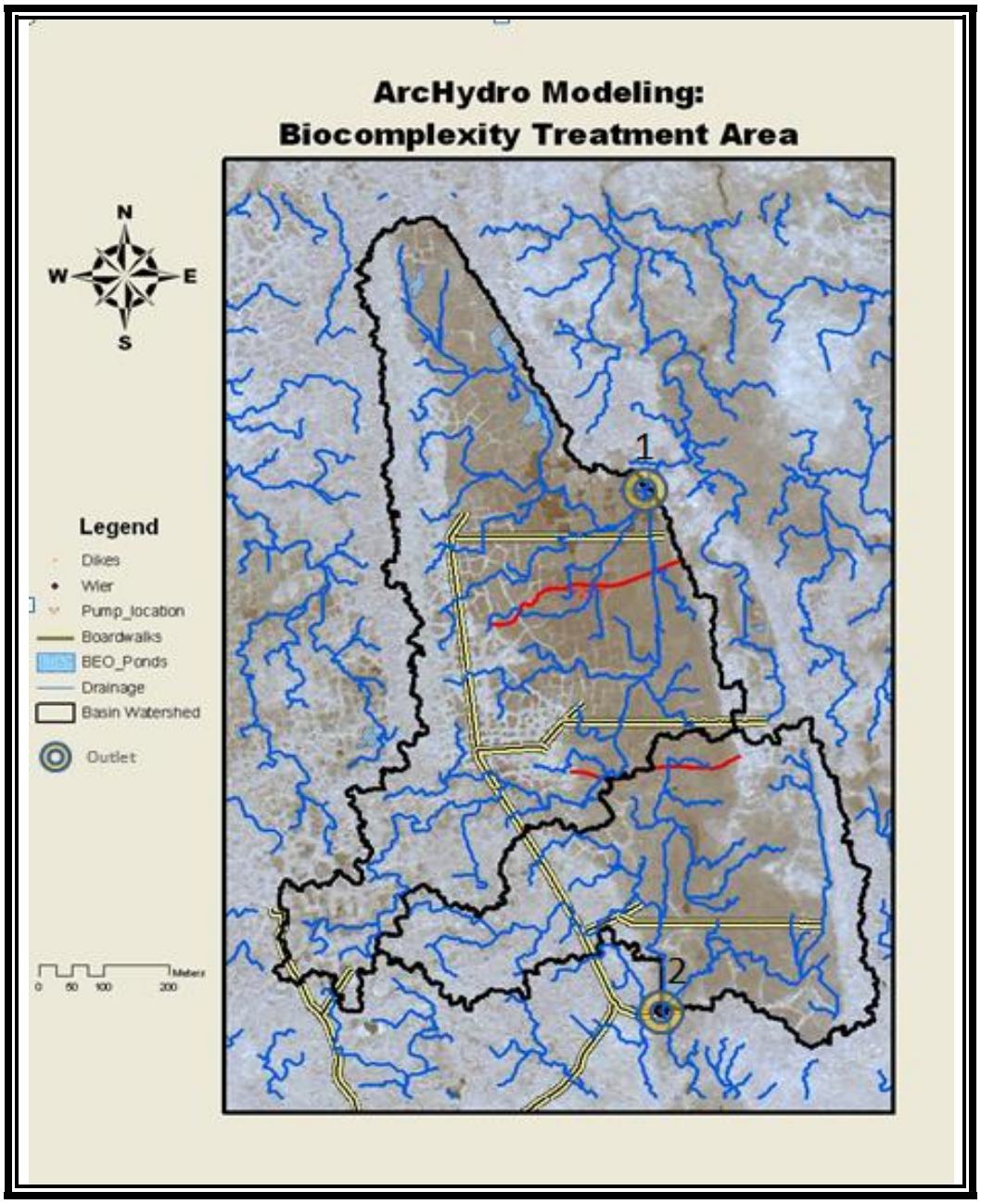

Figure 17. Catchments and drainage of the DTLB. The DTLB used for the Biocomplexity Experiment has two catchments delineated with a black line, a drainage pattern shown with blue lines, and two outlets shown in yellow. The northern outlet 1 was dammed in 2008.

Figure 18 is an illustration showing the modeled drainage lines in blue. These drainage lines occur in between polygon troughs. In flat terrain, the drainage lines cut across the landscape. A zoomed inset on the slope DEM highlights these drainage patterns in detail.

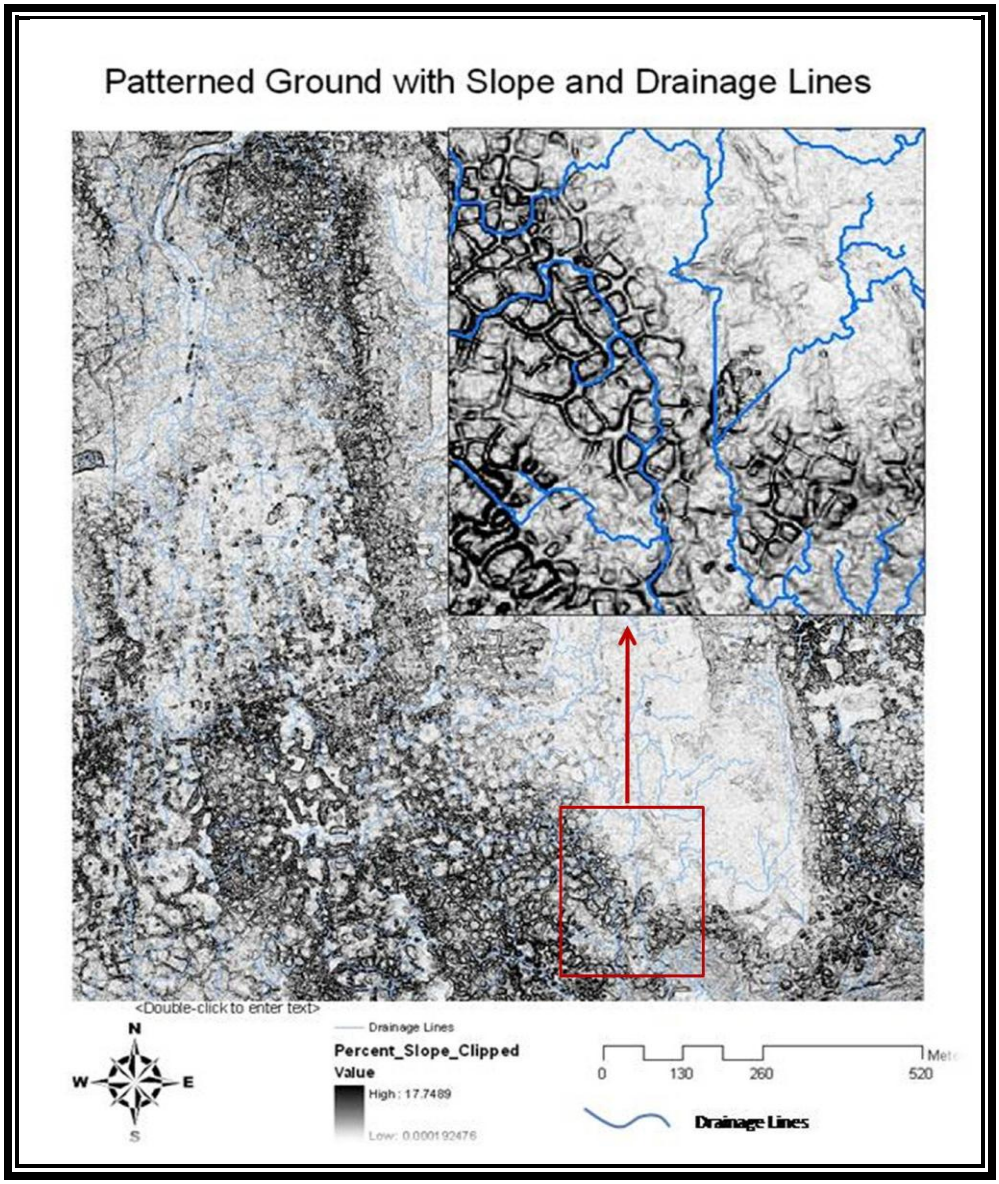

Figure 18. Slope DEM with inset. The inset shows most of the drainage pattern in blue following polygon troughs. On flat terrain, the drainage lines cut across the land.

4.3 Snow Depth and Snow Water Equivalent (SWE) for Spring 2006-2008

Average snow depth and average SWE for all spring field seasons is shown in figure 19. Averaged over all years, snow depth was 43.1cm with a standard deviation of ±15.1cm. Average snow depth for spring 2006 was 44.3cm with a standard deviation of ±13.7cm. Average snow depth was highest in 2007 at 54.6cm with standard deviation of ±21.16cm, whereas 2008 had the least snow depth at 30.5cm with a standard deviation of ±10.5cm.

The average SWE for all field seasons was 10.4cm with a standard deviation of ±3.7cm. SWE was highest in 2007 at 13.9cm with a standard deviation of ±6.9cm, followed by 2006 with SWE at 10.8cm and a standard deviation of ±4.7cm. Spring 2008 had the least SWE at 6.5cm with a standard deviation of ±3.2cm.

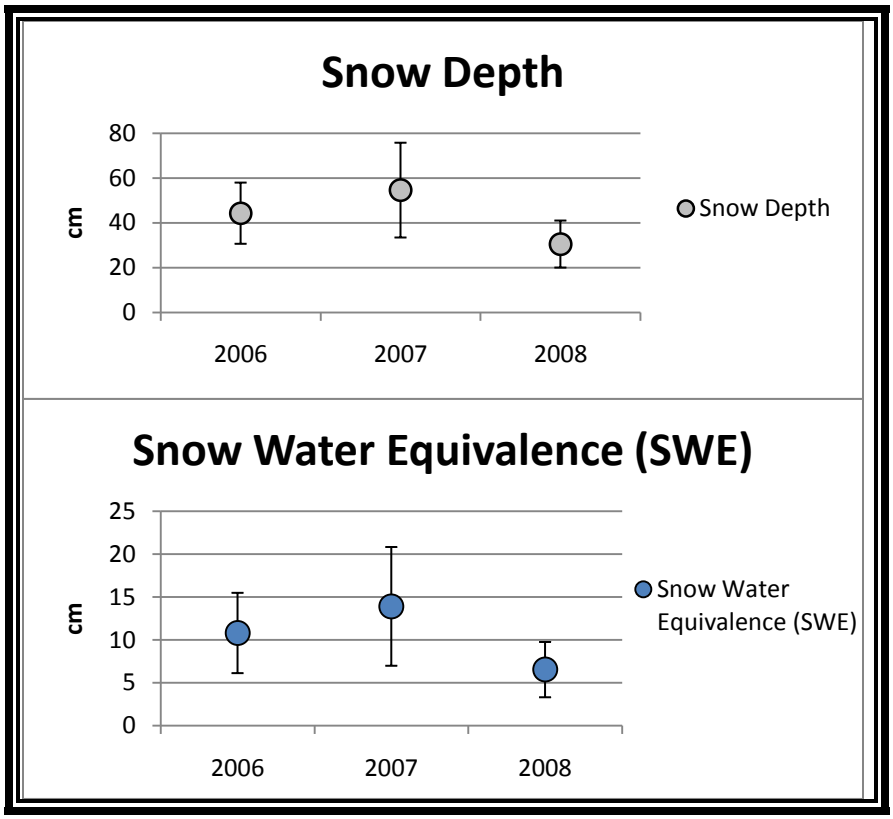

Figure 19. Snow depth and SWE for Spring 2006-2008. Snow depth and SWE show a standard error of ±1.0cm. Snowpack from spring 2007 had the greatest snow depth and snow water equivalency (56.6cm and 13.9cm, respectively). Spring 2008 had the least amount of snow on the ground at 30.5cm.

4.4 Water Table Depth (WTD)

Results for water table depth are shown in Figure 20. Mean seasonal WTD measurements for 2007 and 2008 were calculated for each year and treatment. Overall, water table depth was highest (close to the ground surface) in the flooded treatment and lowest (deepest underground) in the control treatment for summer 2007. In 2008, water table was highest in the flooded treatment, but lowest in the drained treatment. In 2007 (Julian days 170-218), the average WTD for all treatment areas increased 20cm. In 2008 (Julian days 170-200), the average WTD for all treatment areas increased 14cm. .

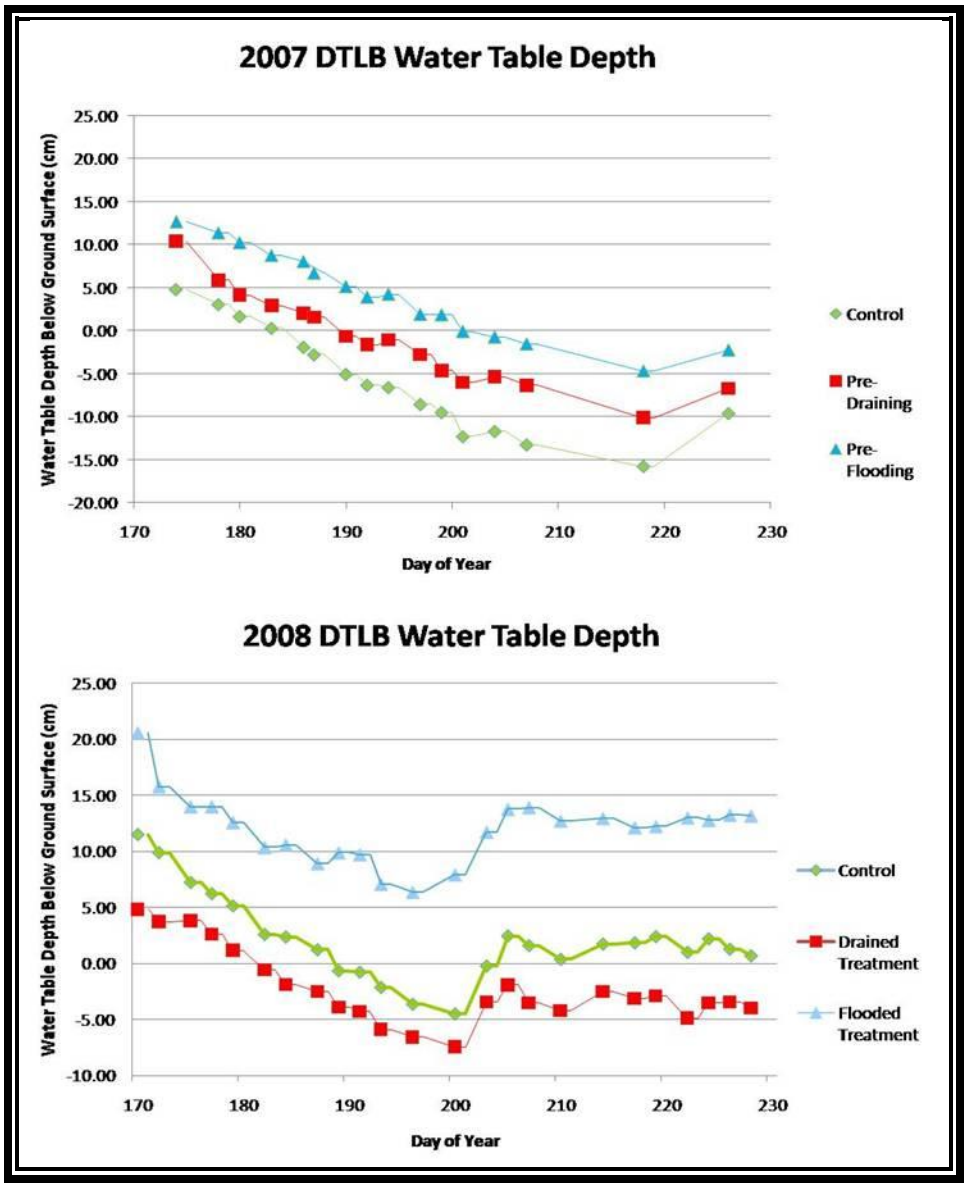

Figure 20. Water table depths for summers 2007-2008. Water table depths are shown for each experimental treatment prior to and during the experimental manipulation. In 2007 (Julian days 170-218), the average water table depth for all treatment areas decreased 20cm. In 2008 (Julian days 170-200), the average water table depth for all treatment areas decreased 14cm.

A Shapiro-Wilk test was performed on the mean differences in WTD between 2007 and 2008. Data were normally distributed ($n=14$, $p>0.05$). The differences in pre and post treatment were analyzed using a two-paired sample t-test and the mean difference in WTD was significantly greater ($p<0.05$) between years for the drained treatment area than for the flooded

as seen in Table 3. These results suggest there was a stronger draining treatment than flooding treatment in 2008 and that the success of the flooding treatment was negligible.

Table 3. Signifcance test for water table depth. A significantly drop in water table depth was observed between 2007 and 2008 for the drained treatment area. No significant difference was observed between 2007 and 2008 for the flooded treatment area.

Two Paired Sample T-Test					
Differences	**(n)**	**Mean**	**Variance**	**T**	**Significance (p<0.05)**
2007 (Control – Drained)	14	-4.6cm	2.3	-18	<0.001
2008 (Control – Drained)	14	3.9cm	0.7		
2007 (Control – Flooded)	14	-9.9cm	2.4	0.2	0.9
2008 (Control – Flooded)	14	-10cm	4.5		

4.5 Thaw Depth

Thaw depth results are illustrated in Figure 21. Thaw depths increased with calendar day in the experimental study site for summers 2007 and 2008. Average maximum thaw depth for all transects in 2007 was 29cm with a standard deviation of ±2.5cm. Average maximum thaw depth for all transects in 2008 was 35cm with a standard deviation of ±3.1cm. Error bars show the standard deviation for each day thaw depth was measured. In 2007, thaw depth for all sampling sites combined increased at a rate of 0.35cm per day, with a standard deviation of ±0.16cm, whereas in 2008, thaw depth increased at a rate of 0.36cm per day with a standard deviation of ±0.28cm.

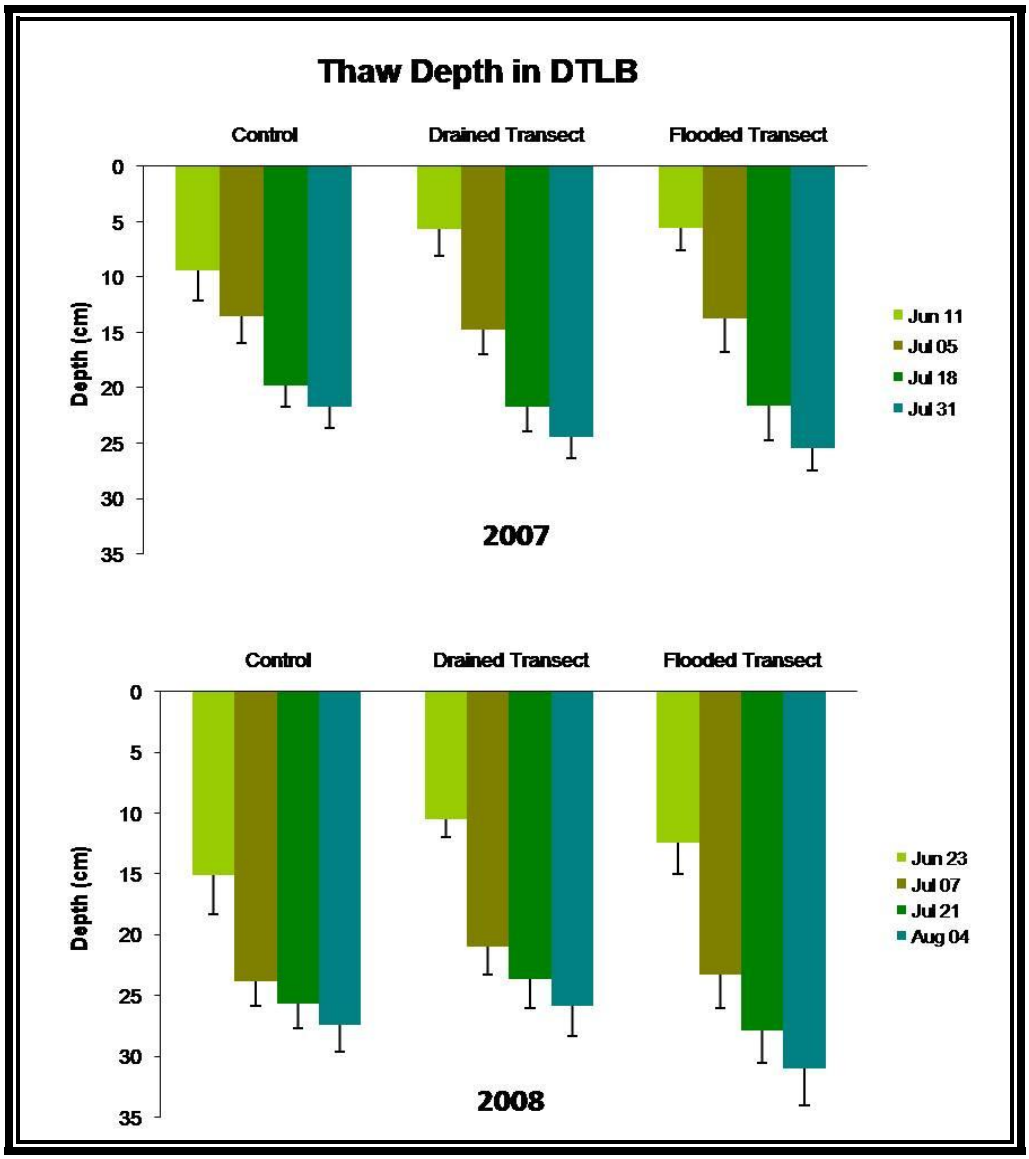

Figure 21. Thaw depths for summers 2007-2008. Seasonal thaw depth increased with calendar day in each experimental treatment in 2007 and 2008. Maximum thaw depth occurred in the flooded transect, with 25cm in 2007 and 34 cm in 2008. Error bars show the standard deviation for each sampling period.

Total season thaw depth data was not normally distributed for summers 2007-2008, as per the Shapiro-Wilk test, ($n=300$, $p<.05$). Therefore, the Wilcoxon Rank Sum test for non-parametric data was used to determine significant differences in pre and post treatment effects. Table 4 shows the results of the Wilcoxon Rank Sum test. The mean difference in thaw depth was significantly lower ($p<0.05$) for the drained treatment area than for the flooded treatment

area in 2008 compared to 2007, as seen in Table 4. Thus, a stronger draining treatment than flooding treatment in 2008 suggests that the flooding treatment was negligible.

Table 4. Wilcoxon rank sum test results for thaw depth. A significant decrease in thaw depth occurred in the drained section in 2008 compared to 2007. Higher thaw depths were observed for the flooded treatment area from 2007 to 2008, but were not significantly different.

Wilcoxon Rank Sum Test			
Differences in Thaw Depths	**(n)**	**Mean**	**Significance ($p<0.05$)**
2007 (Control – Drained)	1200	-0.56cm	< 0.0001
2008 (Control – Drained)	1200	2.78cm	
2007 (Control – Flooded)	1200	-0.48cm	<0.49
2008 (Control – Flooded)	1200	-0.64cm	

4.6 DGPS Water Levels in Ponds

Seasonal pond water level dynamics for sampling periods in 2005-2008 are shown in Figure 22.). Trend lines, shown in red, were used to describe all pond water levels for that season because they provided minimal residuals, though the polynomials were not intended for modeling. In general, all water levels decreased with calendar each season they were monitored. In 2005, water levels peaked at the beginning of the monitoring season, [Julian day 168]. Then pond water levels decreased almost 10cm until [Julian day 178]. A steady state of water levels persisted until [Julian day 194], then a gradual drop of 3cm until Julian day 206 was observed. Summer 2006 had a similar pattern of water level flux to that of 2005. Water levels dropped close to 6cm, between Julian days 167 and 174, and there was a small (≈1cm) increase in water levels between Julian days 178 and 182, then a drop of 5cm by Julian day 199. Water levels began increasing again near Julian day 205 and continued on past Julian day 217. Summer 2007 was very dry, compared to the other field seasons, thus a steady decrease in water levels of about 28cm occurred from Julian day 159 through Julian day 202. There was a slight increase at the end of the summer season. In summer 2008, a gradual drop in pond water levels to that of summer 2007 of about 20cm between Julian day 159 and Julian day 200. A slight increase of 2-3cm was observed toward the end of the field season.

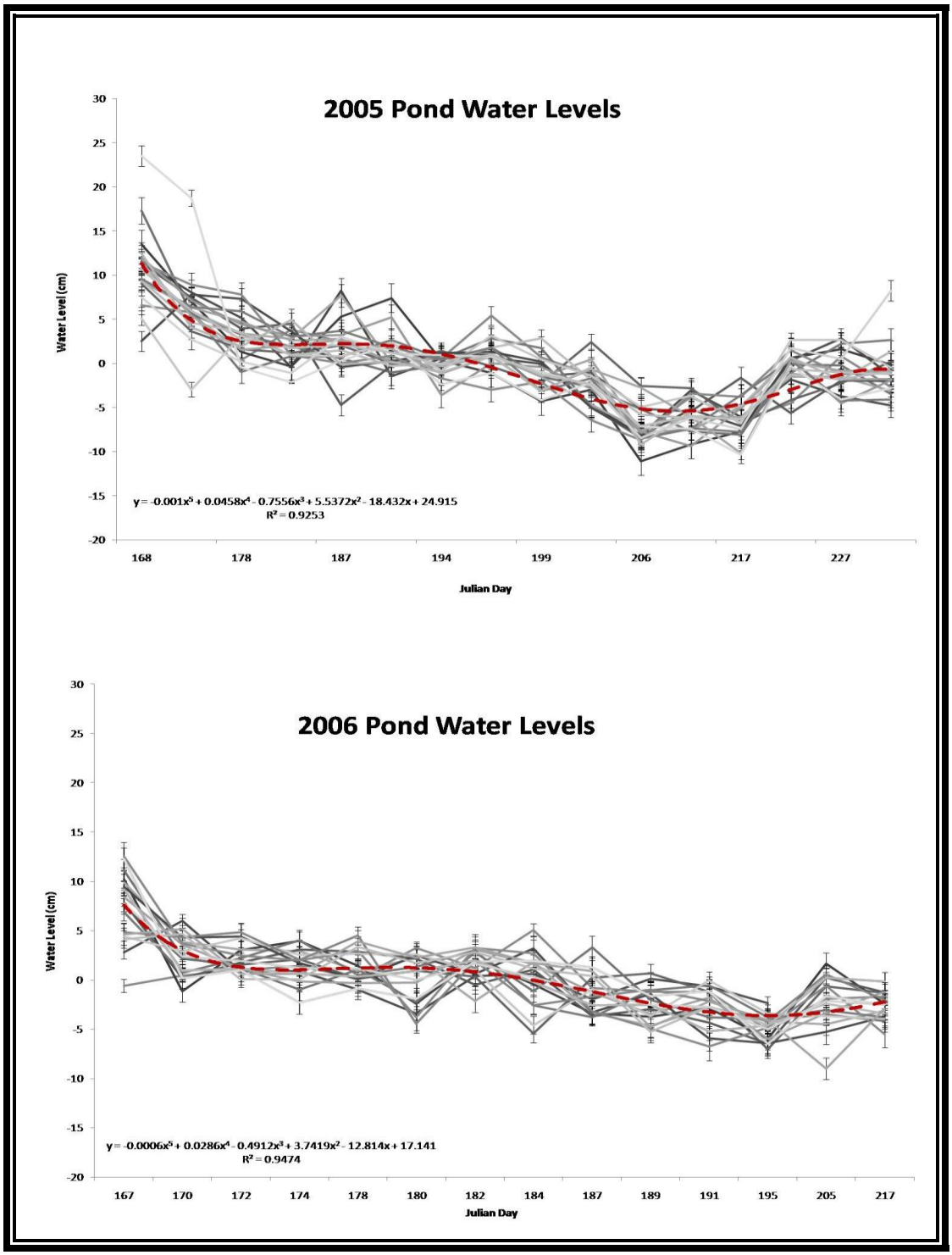
2005 Pond Water Levels
Water Level (cm)
30
25
20
15
10
5
0
-5
-10
-15
-20
y = -0.001x⁵ + 0.0458x⁴ - 0.7556x³ + 5.5372x² - 18.432x + 24.915
R² = 0.9253
168
178
187
194
199
206
217
227
Julian Day
2006 Pond Water Levels
Water Level (cm)
30
25
20
15
10
5
0
-5
-10
-15
-20
y = -0.0006x⁵ + 0.0286x⁴ - 0.4912x³ + 3.7419x² - 12.814x + 17.141
R² = 0.9474
167
170
172
174
178
180
182
184
187
189
191
195
205
217
Julian Day

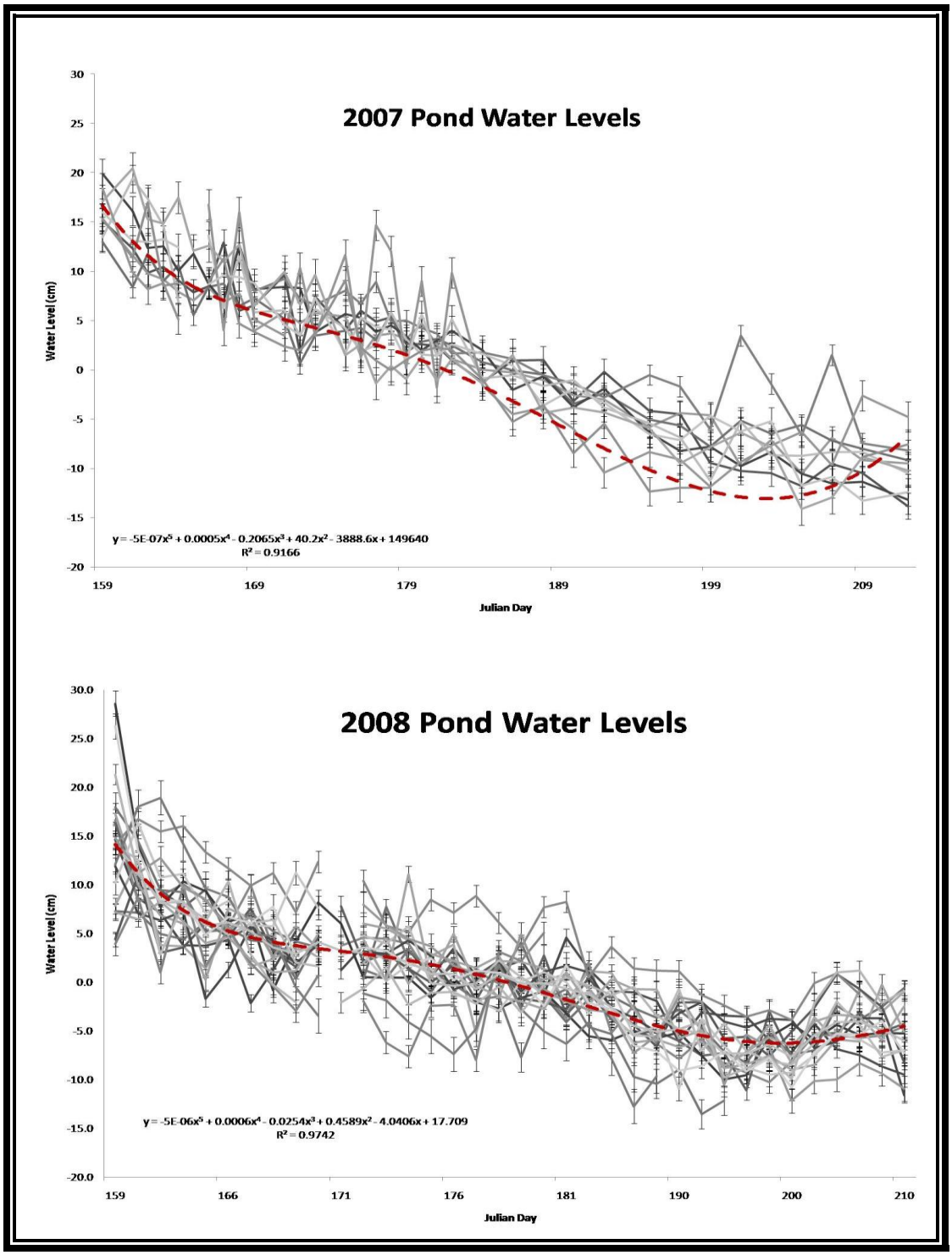

Figure 22. Pond water level trends shown in red for Summers 2005-2008. The lines in red are a best fit 5th order polynomial equation used to describe all pond water levels for that season because they provided minimal residuals, though the polynomials were not intended for modeling. In general, all water levels decline throughout the field season, but can rise with rain events, especially toward the end of the summer season (late July through August). The lines in gray are the individual pond water levels with their respective standard error.

A bivariate x (time) and y (water levels) analysis was performed to achieve a 5^{th} order polynomial shaded confidence curve fit $p<0.05$) for all ponds in a respective year (Figure 23). The water levels were initially normalized by subtracting the initial water level measurement to the next measurement, for all measurements, and dividing by the mean water level for the summer season. The new water level scale allowed for better comparison of all ponds. Summers of 2005 and 2006 were wet years, and therefore have a broad confidence curve fit with an estimated water level range of 15cm. Summer 2007 had virtually no precipitation and a uniform pattern of decreasing water levels is observed for all but one pond that year. Similarly, summer 2008 had a gradual drop in water levels, except for two precipitation events. A small rise in water levels occurred between Julian day 168 and 174, and water levels began rising after Julian day 200. The range of pond water levels for 2007 and 2008 was about 8cm.

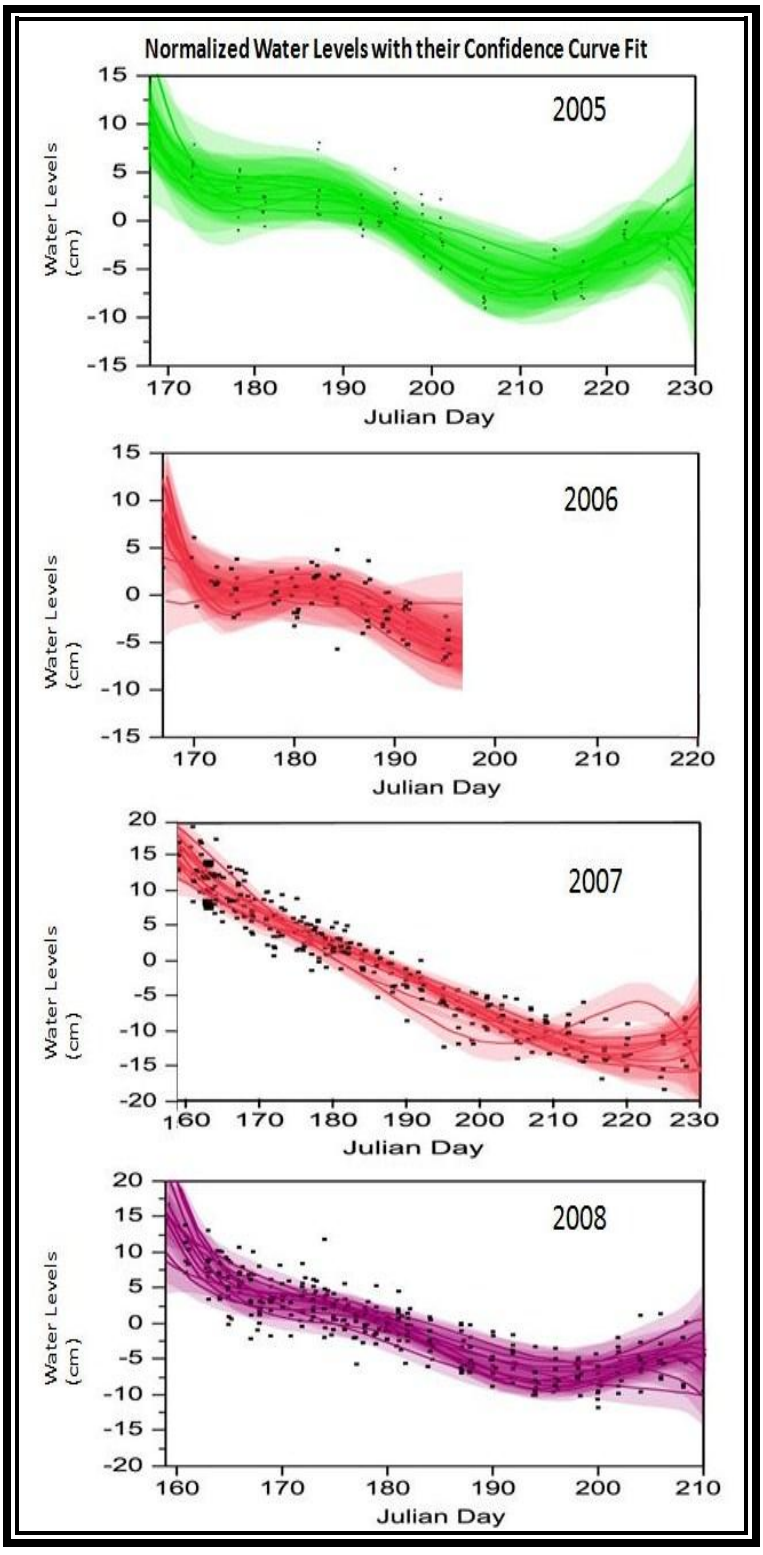

Figure 23. Confidence curve fits for normalized water levels. Shaded curve fits for pond water levels in their respective summer season. The 95% confidence interval indicates that under the same conditions for that particular summer, the pond water levels would fall within that range 95% of the time.

Ponds were separated into their respective treatment areas and their total water levels at the end of the season were averaged out by treatment for 2005-2008, (n=36). Average pond water levels by treatment are plotted in Figure 24. Both control treatments show somewhat of a similar pattern for 2005-2008, unlike the drained and flooded treatments.

In 2005, the drained and flooded treatment water levels (-13.8cm and -13.6cm) were greater than the combined control treatments (-6.2cm). In 2006, the drained treatment water levels (-5.1cm) were less than the flooded treatment (-12.5cm) and combined control treatments (-12.1cm). In 2007, the flooded treatment water levels (-23.6cm) were less than the drained (-29.9cm) and combined control treatments (-29.7cm). By 2008, flooded treatment water levels (-7.7cm) were once again less than the drained treatment (-24.3cm) and the combined control treatments (-19.3cm).

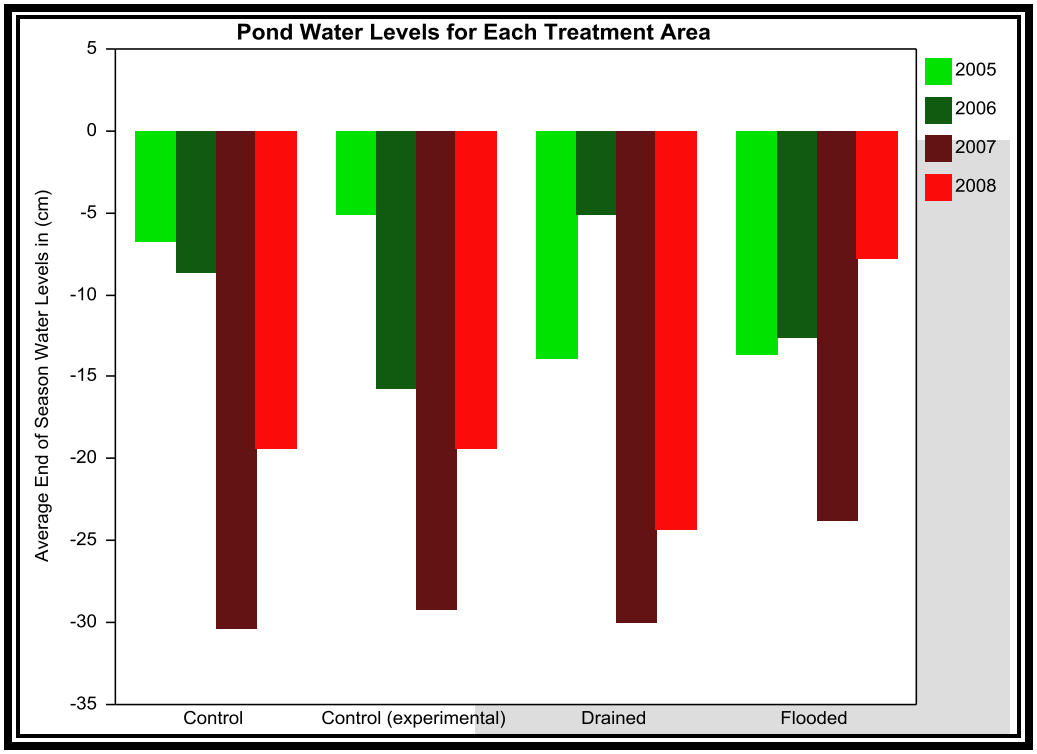

Figure 24. Pond water levels at the end of the field season per their respective treatment and year. The control sections have somewhat of a similar end of season water level, compared to the drained and flooded water levels.

Ponds were analyzed for any possible pre and post treatment effects using a Wilcoxon two-paired signed rank test. The mean differences between each section for all years were compared. Results are shown in Table 5. The success of the flooding and draining treatment was negligible ($p>0.05$). This is in agreement with the confidence curve fits, suggesting that despite the water manipulation, ponds in all treatment areas behaved in a similar fashion.

Table 5. Significance test for pond water levels. The Wilcoxon Rank Sum Test was used for Average Pond Water Levels in Experimental Treatment Areas.

Wilcoxon Rank Sum Test for Ponds (2005-2008)				
Differences in Treatment Areas	**(n)**	**R**	**Mean**	**Significance p<0.05**
Drained -Flooded	4	0.43	-3.89cm	p=0.6
Control (experimental) - Flooded	4	0.54	-2.90cm	p=0.6
Control (outside) - Flooded	4	0.59	-1.83cm	p=0.8
Control (experimental) – Drained	4	0.68	-0.99cm	p=0.8
Control (outside) - Drained	4	0.9	2.06cm	p=0.6
Control (outside) - Control (experimental)	4	0.93	1.08cm	p=1

4.7 HOBO Water Level Logger Data

Summer pond water temperatures recorded from the HOBO water level loggers for 2006 and 2007 were plotted in Figure 24. In 2006, pond temperatures had an average temperature of 8.4ºC with a standard deviation of ±1.7 ºC. The minimum temperature for 2006 occurred in Pond 18 with 5.1 ºC and the maximum temperature was 14.5 ºC in Pond 16. In 2007, pond temperatures were 2 ºC higher, than in 2006, with average pond temperatures at 10.1 ºC, ±1.8 ºC. Pond 16 had the lowest recorded temperature for the season with 5.9 ºC, and Pond 18 had the highest temperature, with 17 ºC.

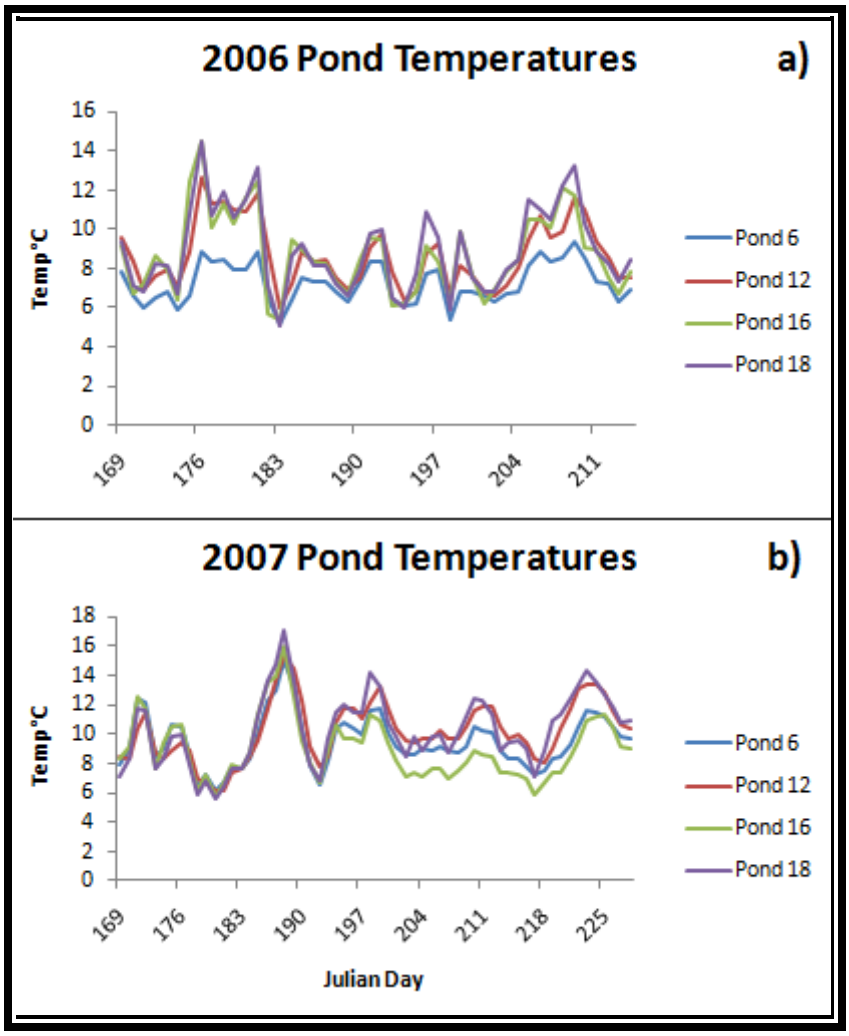

Figure 25. Water temperatures for ponds with level loggers. Ponds 6, 12, 16, and 18 show a similar pattern in water temperature for 2006 (a) and 2007 (b).

Results from the linear regressions with average pond temperatures for 2006 (n=45) and 2007 (n=60) plotted against daily air temperature and solar radiation are shown in Figure 26. The relationship between average pond temperature and air temperature (a and b) was higher for 2006 (R^2=0.62) than for 2007 (R^2=0.57). Similar results were obtained for correlations between average pond temperature and solar radiation in 2006 and 2007 (c and d). However, pond temperature has a stronger relationship with solar radiation in 2007 than in 2006.

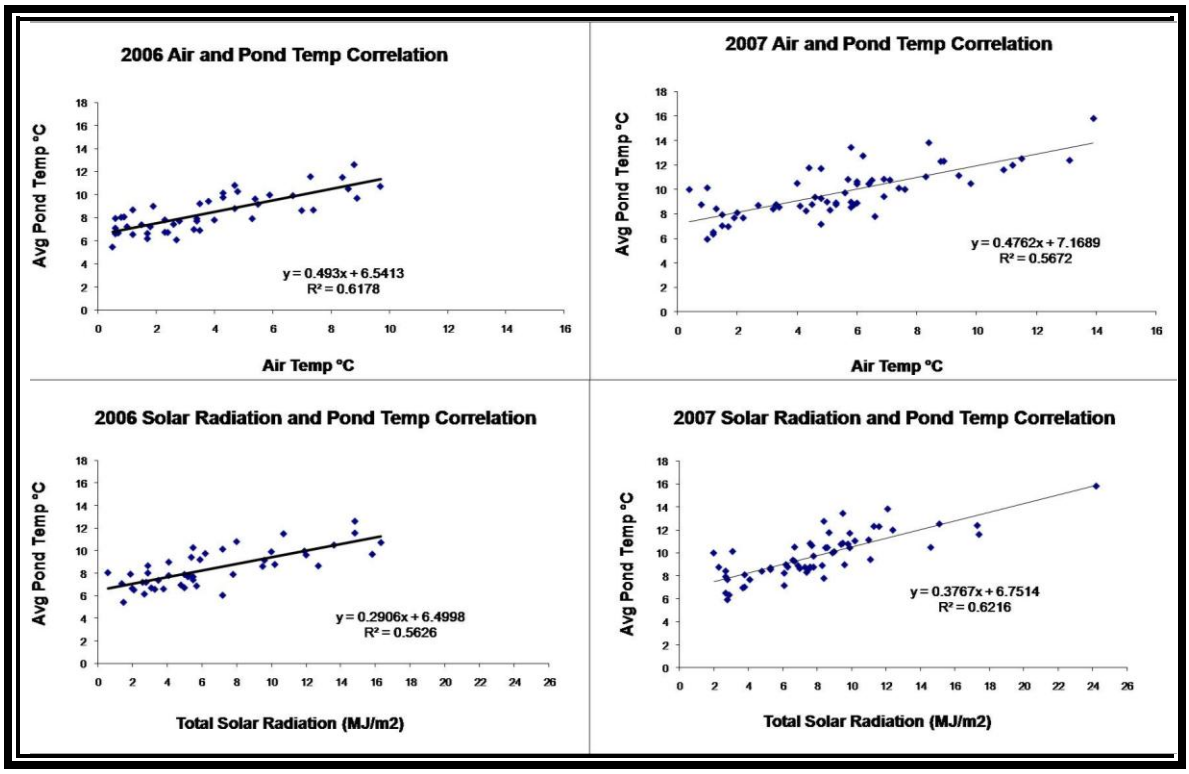

Figure 26. Average pond temperature correlations with atmospheric variables. All correlations were relatively high with R2 > 0.56, ($p<0.05$).

Level logger data shown in Figure 27 is in kPA pressure units and is plotted with precipitation. It is evident from pressure data that ponds respond in a relatively uniform manner to precipitation. Testing of the pumping system in early summer of 2007 may be responsible for the small oscillations from Julian days 167-193. The dry spell of 2007 is also seen by the continuous pressure decrease through time. Pond 6 and Pond 18 are control ponds, whereas Pond 6 is in the flooded treatment area and Pond 16 is in the drained treatment area.

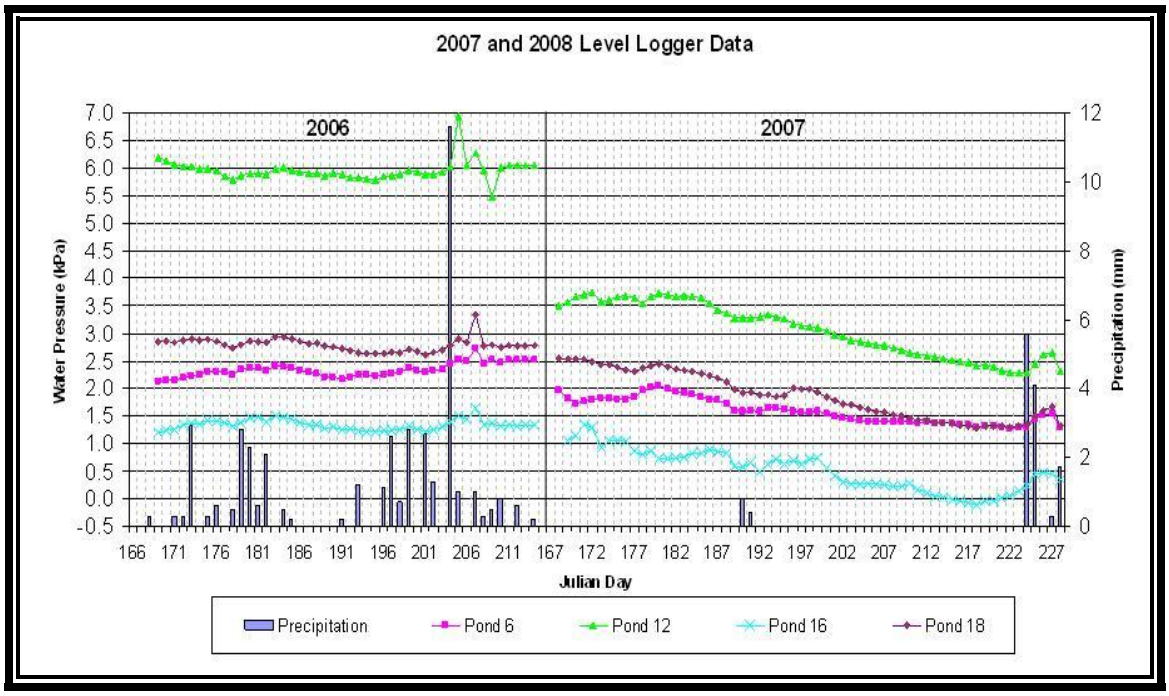

Figure 27. Water pressure in kPA recorded from level loggers. Rain events kept pressure relatively constant in 2006, but the dry summer of 2007 caused a continuous drop in water pressure.

4.8 Evaporation

All pond water temperatures recorded from the level loggers for summers 2006 and 2007 were averaged out per month to calculate evaporation using an empirical equation called Meyer's evaporation formula. The results are shown in Table 6. Overall, evaporation rates were highest during the month of June for 2006 and 2007, with 6.73mm/day and 4.16 mm/day, respectively, compared to July of 2006 and 2007 (2.90 and 3.84 mm/day, respectively) and August 2006 and 2007 (2.52 and 2.23 mm/day, respectively).

Table 6. Daily evaporation rates for summers 2006-2007 in mm/day.

2006	***June***	***July***	***August***
Mean air temp (^{o}C)	2.2	3.3	2.2
Water temp (^{o}C)	9.24	8.13	7.33
Wind Speed (km/hour)	13.55	16.31	14.49
Relative Humidity %	87.86	91.23	81.83
sat. vap. Pressure - e_s (mmHg)	8.87	8.27	7.67
sat. vap. Pressure - e_a (mmHg)	1.93	7.11	6.62
Evaporation (mm/day)	**6.73**	**2.90**	**2.52**
2007	***June***	***July***	***August***
Mean air temp (^{o}C)	1.3	5.7	6.9
Water temp (^{o}C)	8.56	10.19	9.89
Wind Speed (km/hour)	18.42	18.03	15.3
Relative Humidity (%)	90.06	89.77	92.73
sat. vap. Pressure - e_s (mmHg)	8.42	9.77	9.25
sat. vap. Pressure - e_a (mmHg)	4.47	6.08	6.92
Evaporation (mm/day)	**4.16**	**3.84**	**2.23**

Chapter 5: Discussion

The following paragraphs discuss the results from the previous chapter. First, climate data is discussed in 5.1 with short-term noted trends. Patterns observed with the LiDAR DEM and ArcHydro modeling, are discussed in section 5.2. Sections 5.3-5.8 discuss the hydrologic characteristics observed during the four year study, including snow depth and SWE, water table depth, thaw depth, water pressure in ponds, pond temperatures, and evaporation. These hydrologic characteristics are compared to past studies conducted in the Barrow area and other studies related to the Arctic.

5.1 Climate Conditions

Climate data was variable each summer of 2005-2008. Weather in summers of 2005 and 2006 was wet and cool, whereas summer of 2007 was hot and dry. However, the cumulative trend for all summer seasons did indicate warming and drying around the DTLB area. This short term trend is comparable to long-term trends observed in other literature (Curtis *et al.* 1998, Oechel *et al.* 2000).

5.2 LiDAR-derived DEM and ArcHydro Modeling

The LiDAR-derived DEM and associated catchment and drainage characteristics that were modeled displayed a capacity to detect a range features associated with frozen ground such as high and low centered polygons and polygon troughs, tundra ponds and drained thaw lake basins. Long-term changes in these features can indicate ecosystem changes (Stow *et al.* 1989) Scientists have noted polygon troughs to act as flow channels (Woo & Guan 2006), and ArcHydro was able to model such terrain, as seen in figure 18. What is most important is the fine resolution at which the detail was captured with the 1m pixels of the DEM. Many LiDAR studies now use fine spatial resolution of less than 5m (French 2003, Bork & Su 2007, Lee &

Lucas 2007). Although expensive to acquire, LiDAR datasets can improve the quality of DEMs to map remote arctic regions, they improve hydrologic modeling in flat terrain, and build a capacity for monitoring fine-scale change in these landscapes over a variety of spatial and temporal scales (Nolan 2003). Such change is important because micrtopography in arctic terrestrial ecosystems is inextricably linked to soil moisture, depth of thaw, plant community composition and functional variables such as carbon flux (Chapin *et al.* 1997, Hobbie *et al.* 2000, Engstrom *et al.* 2005, Boike *et al.* 2008)

5.3 Snow Depth and Snow Water Equivalent (SWE)

Snow depth and SWE were highly variable in spring of 2006-2008. This variability may be associated with the differences in the time of year snow depth was measured and with the infrastructure that was put in place each year after 2005. Snow accumulation was higher around buildings and boardwalks, as these structures can be similar to snow fences, which block snow from drifting (Hinkel & Hurd 2006). Average snowpack for all field seasons was 43.1cm, and average SWE was 10.4cm and fell within the range commonly reported by other studies in northern Alaskan arctic coastal regions: 52cm snowpack and 13cm SWE (Sturm *et al.* 2001), 28cm snowpack and 9.8cm SWE (Sturm & Liston 2003), 41.3cm snowpack (Hobbie 1980). Annual monitoring of snow depth in late spring is best because snow is not water saturated during this time. Maybe measuring snow depth from a similar DTLB in the surrounding area can also give more accurate measurements, than measuring within the infrastructure found inside the experimental site. Snow depth, though highly variable each year, is important to monitor as snow is the prime source of pond water recharge (Woo & Guan 2006). Decreased winter snow observed in the Barrow region could potentially change pond hydrology affecting permafrost and pond vegetation structure (Hinkel & Hurd 2006).

5.4 Water Table Depth (WTD)

Water table depth increased as the summer season progressed for summer 2007, except toward the end of the season, due to late summer rain events. In 2008, there was a water table increase after Julian Day 200, which might have been caused by failed attempts to conduct the manipulation that year. In order to compare pre and post manipulation changes, the difference in WTD between the flooded/drained treatment areas and the control was compared for summers 2007 and 2008. Results indicate that the difference between the control and drained treatment areas was significant from one year to the next compared to the difference between the control and flooded treatment areas (Table 3). This suggests that water inputs in the flooded treatment did not alter water table depth significantly. However, water removal from the drained treatment altered water table depth significantly. An increasing water table depth means drier organic soils (Boike *et al.* 2008). Increased decomposition of organic matter in dry soils increases the potential for soil organic carbon to be released into the atmosphere, amplifying the positive feedback loop between climate change and atmospheric CO_2 (Hobbie *et al.* 2000).

5.5 Thaw Depth

Thaw depth increased with calendar day during the summers of 2007 and 2008. Average maximum thaw depth in 2007 was 29cm, compared with 35cm in 2008. These differences correspond to 2007 being drier than 2008. The flooded treatment area had the greatest thaw depth in 2007 and 2008, with 32cm and 38cm respectively. Maximum thaw depth in all treatment areas fell within the range given by Hobbie (1980) and Lewellen (1972) in their tundra studies, 20-50cm. Interestingly, Lewellen (1972) reported 1963 to be a very wet year and total thaw depth was 40cm compared to 1964 being a dry year with a total thaw depth of 33cm. Average maximum thaw depths for 2007 and 2008 (32cm) are also comparable to the 7 year

average (31.1cm) reported from 19 US Army Cold Region's Research and Engineering Laboratory (CRREL) plots (Nelson *et al.* 1998) and the 5 year thaw depth average (37cm) reported for the Barrow Circumpolar Active Layer Monitoring (CALM) grid reported by (Hinkel & Nelson 2003).

In order to compare pre and post manipulation changes, the difference in thaw depth between the flooded/drained treatment areas and the control was compared for summers 2007 and 2008. Results indicate that the difference between the control and drained treatment areas was significant from one year to the next, unlike the difference between the control and flooded treatment areas (Table 4). Thaw depth is highly dependent on soil moisture, thus, the drained treatment area had less thaw depth in 2007 because organic soils were dry enough to act as efficient thermal insulators against temperature forcing (Hinkel *et al.* 2001). If the warming and drying trends were to continue in Barrow, one could expect less thaw depth (Zhang & Stammes 1998). However, Hinkel et al. (2001) conclude that there is high variability in thaw depth within the Barrow microtopography, and they caution about extrapolating to larger scales.

5.6 Water Levels in Ponds

Water levels overall decreased with calendar day during the summer field seasons of 2005-2008 as seen in Figures 22 and 23. After the spring freshet, most ponds behaved in a synchronous fashion, with slight increase in water levels after rain events, especially toward the end of the field seasons, which implies that they are hydrologically disconnected, act as their own micro-catchments, and are most likely impacted primarily by evaporation, as observed in other arctic pond and lake studies (Hobbie 1980, Miller *et al.* 1980, Marsh *et al.* 1981, Macrae *et al.* 2004, Woo & Guan 2006).

One factor that is unknown in pond water levels, especially during dry years like 2007 is how much ground ice contributes to water storage and vegetation growth (Young 2006), since thaw depth lessens when dry conditions occur. Overall, ponds and wetlands in continuous permafrost and highly dependent on precipitation and may be most vulnerable to climate change, as their drying can lead to pond depletion and CO_2 and CH_4 release into the atmosphere, enhancing the positive feedback to global warming (Burkett & Kusler 200, Winter 2000).

5.7 Water Level Logger Data

Pond water temperatures recorded from the HOBO water level loggers for summers 2006 and 2007 (8.4ºC and 10.1 ºC, respectively) were slightly lower than the average pond water temperatures reported in by Lewellen (1972) in 1965 (10.3ºC) and higher than what he reported in 1966 (6.6 ºC). However, the HOBO logger temperatures were slightly higher than the pond temperatures reported in the early 1970's (Miller *et al.* 1980), which had average pond temperatures between 7 ºC to 8ºC. Results from the linear regressions with average pond temperatures for 2006 and 2007 plotted against daily air temperature and solar radiation show a relatively strong relationship. However, pond temperatures had a stronger relationship with solar radiation in 2007 than in 2006 because 2006 was a wet year with more cloud cover, thus temperature forcing was greater than solar radiation forcing on pond temperatures for that year (Miller *et al.* 1980).

5.8 Evaporation

Evaporation rates were higher in June of 2006 and 2007, with average evaporation of 5.4mm/day for both years, compared to July and August of 2006 and 2007 (3.15mm/day and 2.4mm/day, respectively). Average evaporation for June and July of 2006 and 2007 was higher

than the evaporation rate reported for a shallow lake in the Mackenzie Delta (Marsh 1986). However, the evaporation rate for August in Barrow (2.4mm/day) was very similar to the August evaporation rate in the Mackenzie Delta (2.1mm/day). Average summer evaporation rates for 2006 and 2007 combined (3.65mm/day) were lower than the average evaporation rates (4.3mm/day) reported from ponds in Barrow, AK, (Brown 1980), but similar to the modeled average evaporation rates (31.mm/day) reported by Mendez et. al. (1998) for ponds near Prudhoe Bay. Mendez et al. concluded that coupling of warmer air temperatures with more precipitation could lead to increased evapotranspiration rates, which is not the current trend.

Differences in evaporation rates may be due to several factors. Evaporation formulas being used have coefficients that vary, depending on the size of a water body, or climatic factors (Shnitnikov 1974, Mendez *et al.* 1998, Subramanya 2008). Also, many studies presenting the evaporation regime of a catchment actually calculate evapotranspiration rates from soil water content and vegetation. Evapotranspiration from vegetation and land is estimated to be about 50-80% of total evaporation from open water, thus inter-comparison between studies can be difficult or misleading (Clebsch & Shanks 1957). To a lesser extent, differences in soil substrate or latitude location may also affect evaporation rates.

This thesis presents many patterns and characteristics for the hydrology in the Biocomplexity study site. For future work, developing a drainage and catchment model before conducting any study is greatly advised, as field researchers can ground-truth part of what is being modeled prior to conducting any experiments. Another way to improve future quantity and quality of hydrologic data collection in would be to include the freeze-back period (Young 2006), at least until mid September to double-check for hydrologic connectivity amongst ponds as water levels rise in late summer and to gather somewhat more of a long-term dataset for

studying multiple parameters over multiple years, avoiding gaps between summer seasons. With more efficient use of time, a water balance could be performed to compare with other studies (Hobbie 1980, Marsh 1986, Mendez *et al.* 1998).

Chapter 6: Conclusion

This thesis successfully illustrates multiple hydrologic variables present in the study site as discussed in the previous chapter for snow depth and SWE, water table depth, thaw depth, pond water levels, pond pressure and temperature, and evaporation. The drainage and catchments were also successfully modeled, although time consuming for a novice using the ArcGIS software and ArcHYDRO tools.

Overall, the results from the hydrologic variables observed seem to fall in line with past and present studies. A closer analysis of pre and post treatment effects for water table depth and thaw depth reveal that the draining effect was significantly more effective than the flooding treatment in relation to the controls. For the water table depth plot, the flooding treatment might have been stronger toward the end of the summer as the water table dipped and then flattened out. Reported over-pumping may have caused overflow in the flooded treatment area, thus improvement of the pumping infrastructure is suggested.

Many arctic studies, including this thesis. noted high variability from one year to the next in multiple hydrology parameters, which adds complexity to the many biogeophysical processes already taking place in the coastal plains near Barrow, Alaska. In long-term trends however, the conceptual model in Figure 28 illustrates the basic interactions between climate, hydrology, and land-atmosphere feedbacks to the climate system.

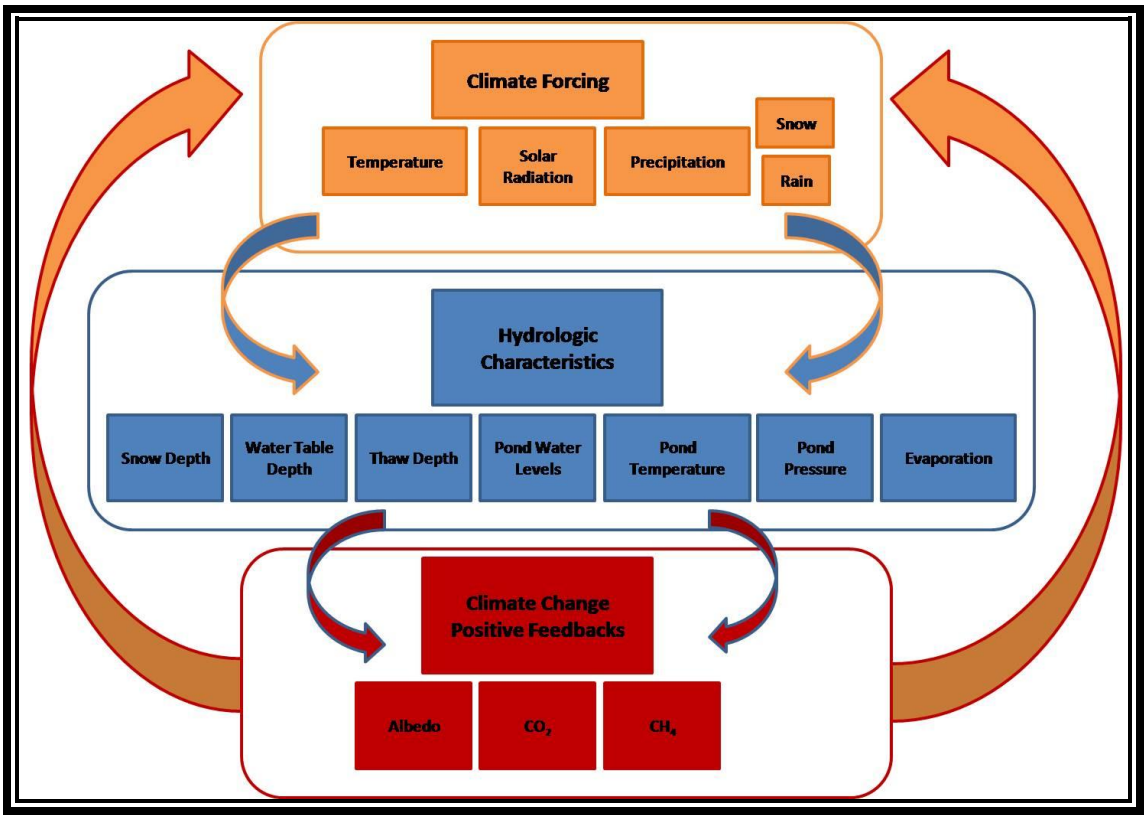

Figure 28. Conceptual Model of the links between climate forcing, hydrology, and climate change positive feedbacks. These links are representative of the coastal plain near Barrow, Alaska.

In Barrow, the warming and drying trend means a potential loss of soil water content and a decreasing water table, as observed in the draining treatment. Warming of the soils can heighten decomposition of organic matter, hence an increase in CO2 gas into the atmosphere, positively enhancing greenhouse warming. Although drying of soils can increase decomposition rates due to increased aerobic volume in tundra soils, dry soils can efficiently insulate against atmospheric heat, thus it is believed that this process can redirect carbon nutrients further down the soil column.

Although difficult and expensive, only long-term continuous monitoring in these extreme and remote locations will help in better understanding the complex land-water-atmosphere interactions and feedbacks in arctic terrestrial ecosystems to more accurately predict future climate impacts.

References

ACIA (2005). Cambridge University Press, Cambridge.

Aguirre A, Brown J, Gaylord A, Tweedie CE (2008) In: *Ninth International Conference on Permafrost*, Vol. 1 (ed Kane D. HKM), pp. 5. Institute of Northern Engineering, Fairbanks, Alaska.

ARCUS (1999). Fairbanks, AK.

Arge L, Chase JS, Halpin P, Toma L, Vitter JS, Urban D, Wickremesinghe R (2003) Efficient flow computation on massive grid terrain datasets. *Geoinformatica,* **7**, 283-313.

Bockheim JG (2007) Importance of cryoturbation in redistributing organic carbon in permafrost-affected soils. *Social Science Society of America Journal,* **71**, 1331-1342.

Bockheim JG, Everett LR, Hinkel KM, Nelson FE, Brown J (1999) Soil organic carbon storage and distribution in arctic tundra, barrow, alaska. *Soil Science Society of America Journal,* **63**, 934-940.

Bockheim JG, Hinkel KM (2007) The importance of "Deep" Organic carbon in permafrost-affected soils of arctic alaska. *Soil Science Society of America Journal,* **71**, 1889-1892.

Boike J, Wille C, Abnizova A (2008) Climatology and summer energy and water balance of polygonal tundra in the lena river delta, siberia. *Journal of Geophysical Research,* **113**, 15.

Bork EW, Su JG (2007) Integrating lidar data and multispectral imagery for enhanced classification of rangeland vegetation: A meta analysis. *Remote Sensing of Environment,* **111**, 11-24.

Bowling LC, Kane DL, Gieck RE, Hinzman LD, Lettenmaier DP (2003) The role of surface storage in a low-gradient arctic watershed. *Water Resources Research,* **39**, 13.

Brown J (1980) *An arctic ecosystem : The coastal tundra at barrow, alaska* Dowden, Hutchinson & Ross :, Stroudsburg, PA.

Brown J, Miller PC, Tieszen L, Bunnell FL (1980) *An artic ecosystem: The coastal tundra at barrow, alaska.* Dowden, Hutchinson and Ross, Inc., Stroudsburg, Pennsylvania.

Burkett V, Kusler J (200) Climate change: Potential impacts and interactions in wetlands of the united states. *Journal of the American Water Resources Association,* **36**, 313-320.

Callaghan TV, Bjorn LO, Chernov Y*, et al.* (2004c) Effects of changes in climate on landscape and regional processes, and feedbacks to the climate system. *Ambio,* **33**, 459-468.

Chapin FS (1993) Environmental responses of plants and ecosystems as predictors of the impact of global change. *Journal of Biosciences,* **18**, 515-524.

Chapin FS, III, Sturm M, Serreze MC*, et al.* (2005) Role of land-surface changes in arctic summer warming. *Science,* **310**, 657-660.

Chapin FS, McFadden JP, Hobbie SE (1997) The role of arctic vegetation in ecosystem and global processes. In: *Ecology of arctic environments* (eds Woodin SH, Marquiss M), pp. 97-109. Blackwell Science Ltd., Malden, MA.

Christensen TR, Friborg T, Johansson M (2008) In: *Ninth International Conference on Permafrost (NICOP)*, Vol. 1 (ed Kane D. HKM). Institute of Northern Engineering, University of Alaska Fairbanks, University of Alaska, Fairbanks, Alaska.

Clawges R, Vierling K, Vierling L, Rowell E (2008) The use of airborne lidar to assess avian species diversity, density, and occurrence in a pine/aspen forest. *Remote Sensing of Environment,* **112**, 2064-2073.

Clebsch ECC, Shanks RE (1957). University of Tenessee, Knoxville, TN.

Curtis J, Wendler G, Stone R, Dutton E (1998) Precipitation decrease in the western arctic, with special emphasis on barrow and barter island, alaska. *International Journal of Climatology,* **18**, 1687-1707.

Donnellan A, Zebker H, Ranson KJ (2008) Radar and lidar measurement of terrestrial processes. *EOS, Transactions, American Geophysical Union,* **89**, 2.

Engstrom R, Hope A, Kwon H, Stow D, Zamolodchikov D (2005) Spatial distribution of near surface soil moisture and its relationship to microtopography in the alaskan arctic coastal plain. *Nordic Hydrology,* **36**, 219-234.

ESRI (2007). ESRI Press, Redlands, CA.

Fitzpatrick EA (1997) Arctic soils and permafrost. In: *Ecology of arctic environments: 13th special symposium of the british ecological society* (eds Woodin SJ, Marquiss M), pp. 292. University Press, Cambridge.

French JR (2003) Airborne lidar in support of geomorphological and hydraulic modelling. *Earth Surface Processes and Landforms,* **28**, 321-335.

Group NWW (1988) In: *AMAP Assessment Report: Arctic Pollution Issues (AAR Figure 2.13)*, pp. 452. Sustainable Development Branch, Environment Canada., Montreal, Quebec.

Hinkel KM, Eisner WR, Bockheim JG, Nelson FE, Peterson KM, Dai XY (2003) Spatial extent, age, and carbon stocks in drained thaw lake basins on the barrow peninsula, alaska. *Arctic Antarctic and Alpine Research,* **35**, 291-300.

Hinkel KM, Hurd JK (2006) Permafrost destabilization and thermokarst following snow fence installation, barrow, alaska, USA. *Arctic Antarctic and Alpine Research,* **38**, 530-539.

Hinkel KM, Nelson FE (2003) Spatial and temporal patterns of active layer thickness at circumpolar active layer monitoring (calm) sites in northern alaska, 1995-2000. *Journal of Geophysical Research,* **108**, 13.

Hinkel KM, Paetzold F, Nelson FE, Bockheim JG (2001) Patterns of soil temperature and moisture in the active layer and upper permafrost at barrow, alaska: 1993-1999. *Global and Planetary Change,* **29**, 293-309.

Hinzman LD, Bettez ND, Bolton WR*, et al.* (2005) Evidence and implications of recent climate change in northern alaska and other arctic regions. *Climatic Change,* **72**, 251-298.

Hobbie JE (1975) In: *Proceedings of the Circumpolar Conference on Northern Ecology*, pp. 43-51. Ottowa, Canada.

Hobbie JE (1980) *Limnology of tundra ponds, barrow, alaska.* Dowden, Hutchinson & Ross, Stroudsburg, Pa.

Hobbie SH, Schimel JP, Trumbore SE, Randersons JR (2000) Controls over carbon storage and turnover in high-latitude soils. *Global Change Biology,* **6**, 196-210.

Hollister RD, Webber PJ, Nelson FE, Tweedie CE (2006) Soil thaw and temperature response to air warming varies by plant community: Results from an open-top chamber experiment in northern alaska. *Arctic, Antarctic, and Alpine Research,* **38**, 206-215.

IPCC (2007) In:

(ed Solomon S, D. Qin, M. Manning, Z. Chen, M. Marquis, K.B. Averyt, M. Tignor and H.L. Miller).

Joabsson A, Christensen TR, Wallén B (1999) Vascular plant controls on methane emissions from northern peatforming wetlands. *Trends in Ecology & Evolution,* **14**, 385-388.

Jordan TE, Lloyd AH, McClelland JW, Langdon C, Moutat DA, Havstad KM, MacMahon JA (2007), Vol. February 2007. Association of Ecosystem Research Centers.

Jorgenson MT, Racine CH, Walters JC, Osterkamp TE (2001) Permafrost degradation and ecological changes associated with a warming climate in central alaska. *Climatic Change,* **48**, 551-579.
Judd KE, Kling GW (2002) Production and export of dissolved c in arctic tundra mesocosms: The role of vegetation and water flow. *Biogeochemistry,* **60**, 213-234.
Kane D, Hinzman L, Woo MK, Everett KR (1992) Arctic hydrology and climate change. In: *Arctic ecosystems in a changing climate: An ecophysiological perspective* (eds Chapin FS, Jefferies RL, Reynolds JF, Shaver GR, Svoboda J). Academic Press, Inc., San Diego.
Kane DL, Gieck RE, Hinzman LD (2008) In: *Ninth International Conference on Permafrost (NICOP)*(ed Kane D. HKM), pp. 883-888. Institute of Northern Engineering, Fairbanks, Alaska.
Lee AC, Lucas RM (2007) A lidar-derived canopy density model for tree stem and crown mapping in australian forests. *Remote Sensing of Environment,* **111**, 493-518.
Lefsky MA, Cohen WB, Parker GG, Harding DJ (2002) Lidar remote sensing for ecosystem studies. *Bioscience,* **52**, 19-30.
Lewellen RI (1972) *Studies on the fluvial environment, arctic coastal plain province, northern alaska.* self-published, Littleton, CO.
Luo Y, Gavrilova ML (2006) 3d building reconstruction from lidar data. *Computational Science and Its Applications - Iccsa 2006, Pt 1,* **3980**, 431-439.
Macrae ML, Bello RL, Moot LA (2004) Long-term carbon storage and hydrological control of co2 exchange in tundra ponds in the hudson bay lowland. *Hydrological Processes,* **18**, 2051-2069.
Maidement DR (Ed.) (2002) *Arc hydro; gis for water resources,* ESRI Press, Redlands, CA.
Marsh P (1986) In: *Symposium: Cold Regions Hydrology*(ed D. K). American Water Resources Association, Fairbanks, Alaska.
Marsh P, Rouse WR, Woo M (1981) Evaporation at a high arctic site. *Journal of Applied Meteorology,* **20**, 713-716.
McGuire AD, Anderson LG, Christensen TR*, et al.* (2009) Sensitivity of the carbon cycle in the arctic to climate change. *Ecological Monographs,* **79**, 523-555.
Mendez J, Hinzman LD, Kane DL (1998) Evapotranspiration from a wetland complex on the arctic coastal plain of alaska. *Nordic Hydrology,* **29**, 303-330.
Miller MC, Prentki RT, Barsdate RJ (1980) Physics. In: *Limnology of tundra ponds, Barrow, Alaska* Vol. 13 (ed Hobbie JE), pp. 514. Dawders, Hutchinson, & Ross, Straudsburg, PA.
National Wetlands Working Group (1988) In: AMAP Assessment Report: Arctic Pollution Issues (AAR Figure 2.13), pp. 452. Sustainable Development Branch, Environment Canada, Montreal, Quebec.
Nelson FE, Anisimov OA, Shiklomanov NI (2002) Climate change and hazard zonation in the circum-arctic permafrost regions. *Natural Hazards,* **26**, 203-225.
Nelson FE, Brown J, Lewkowicz T, Taylor A (2007) Circimpolar Active Layer Monitoring (CALM): Active Layer Protocol.
Nelson FE, Outcalt SI, Brown J, Shiklomanov NI, Hinkel K (1998) Spatial and temporal attributes of the active-layer thickness record. In: *Seventh International Conference on Permafrost*, Vol. 55. Collection Nordicana, Yellowknife, Canada.
NOAA (2006). NOAA Online Weather Data: 1971-2000. Fairbanks, AK.
Nolan M (2003) IPY: An excellent opportunity to improve Arctic DEMs and document today's Arctic for future generations. In: *AGU*, Vol. Abstract #C41C-0991. AGU, San Francisco.

Oberbauer SF, Tweedie CE, Welker JM, *et al.* (2007) Tundra CO_2 fluxes in response to experimental warming across latitudinal and moisture gradients. *Ecological Monographs,* **77**, 221-238.

Oechel WC, Vourlitis GL, Hastings SJ, Bochkarev SA (1995) Change in arctic CO_2 flux over 2 decades - effects of climate-change at Barrow, Alaska. *Ecological Applications,* **5**, 846-855.

Oechel WC, Vourlitis GL, Hastings SJ, Zulueta RC, Hinzman L, Kane D (2000) Acclimation of ecosystem CO_2 exchange in the Alaskan arctic in response to decadal climate warming. *Nature,* **406**, 978-981.

Olsson PQ, Sturm M, Racine CH, Romanovsky V, Liston GE (2003) Five stages of the Alaskan arctic cold season with ecosystem implications. *Arctic Antarctic and Alpine Research,* **35**, 74-81.

Ping CL, Lynn LA, Michaelson GJ, Jorgenson MT, Shur YL, Kanevskiy M (2008) Classification of Arctic tundra soils along the Beaufort sea coast, Alaska. In: *Ninth International Conference on Permafrost (NICOP)*, Vol. 2 (ed Kane D.L. HKM). Institute of Northern Engineering, University of Alaska Fairbanks, Fairbanks, Alaska.

Richter-Menge J, Overland J, Proshutinsky A, *et al.* (2006) State of the Arctic Report. Seattle, WA.

Richter-Menge J, Overland J, Svoboda M, *et al.* (2008) Arctic report card 2008. Seattle, WA.

Ritter DF, Kochel RC, Miller JR (2002) *Process geomorphology.* McGraw-Hill, New York.

Romanovsky V, Burgess M, Smith S, Yoshikawa K, Brown J (2002) Permafrost temperature records: Indicators of climate change. *EOS, Transactions, American Geophysical Union,* **83**, 589.

Schuur EAG, Bockheim J, Canadell JG, *et al.* (2008) Vulnerability of permafrost carbon to climate change: Implications for the global carbon cycle. *Bioscience,* **58**, 701-714.

SEARCH (2005) Study of environmental arctic change; plans for implementation during the Inernational Polar Year and Beyond. In: *Study of Environmental Change*, pp. 104. Arctic Research Consortium of the United States, Fairbanks, AK.

Serreze MC, Francis JA (2006) The arctic amplification debate. *Climatic Change,* **76**, 241-264.

Shnitnikov AV (1974) Current methods for the study of evaporation from water surfaces and evapotranspiration. *Hydrological Sciences Journal,* **19**, 85-97.

Smith LC, Sheng Y, MacDonald GM, Hinzman LD (2005) Disappearing Arctic lakes. *Science,* **308**, 1429-1429.

Smol JP, Douglas MSV (2007) Crossing the final ecological threshold in high arctic ponds. *Proceedings of the National Academy of Sciences of the United States of America,* **104**, 12395-12397.

Stafford JM, Wendler G, Curtis J (2000) Temperature and precipitation of Alaska: 50 year trend analysis. *Theoretical and Applied Climatology,* **67**, 33-44.

Stone RS, Dutton EG, Harris JM, Longenecker D (2002) Earlier spring snowmelt in northern alaska as an indicator of climate change. *Journal of Geophysical Research-Atmospheres,* **107**, 14.

Stow D, Burns B, Hope A (1989) Mapping arctic tundra vegetation types using digital spot/hrv-xs data a preliminary assessment. *International Journal of Remote Sensing,* **10**, 1451 - 1457.

Streutker DR, Glenn NF (2006) Lidar measurement of sagebrush steppe vegetation heights. *Remote Sensing of Environment,* **102**, 135-145.

Sturm M, Liston GE (2003) The snow cover on lakes of the arctic coastal plain of Alaska, USA. *Journal of Glaciology,* **49**, 370-380.
Sturm M, McFadden JP, Liston GE, Chapin FS, Racine CH, Holmgren J (2001) Snow-shrub interactions in arctic tundra: a hypothesis with climatic implications. *Journal of Climate,* **14**, 336-344.
Sturm M. RC, Tape K. (2001) Increasing shrub abundance in the Arctic. *Nature,* **411**, 546-547.
Subramanya K (2008) *Engineering hydrology.* Tata McGraw-Hill Company, New Delhi.
Tarnocai C, Broll G (2008) Soil organic carbon stocks in the northern permafrost region and their role in climate change. In: *Ninth International Conference on Permafrost (NICOP)*, Vol. 2 (ed Kane D. HKM). Institute of Northern Engineering, Fairbanks, Alaska.
Tweedie CE, Gaylord A (2006). National Snow and Ice Data Center, Digital Media., Boulder, CO.
UIC (2003). Reflections; 2003 Annual Report. Barrow, Alaska.
US Arctic Research Commission Permafrost Task Force (2003) Climate Change, Permafrost, and Impacts on Civil Infrastructure. Special Report (eds Nelson FE, Brigham LW). U.S. Arctic Research Commission, Arlington, Virginia.
Walker DA, Raynolds MK, Daniëls FJ*, et al.* (2005) The circumpolar arctic vegetation map. *Journal of Vegetation Science,* **16**, 267-282.
Washburn AL (1980) *Geocryology, a survey of periglacial processes and environments.* John Wiley & Sons, New York.
Webber PJ, Walker MD (1991) International Tundra Experiment (ITEX): Resolution. *Arctic and Alpine Research,* **23**, 124.
Winter TC (2000) The vulnerability of wetlands to climate change; a hydrological landscape perspective. *Journal of the American Water Resources Association,* **36**, 305-311.
Woo MK, Guan XJ (2006) Hydrological connectivity and seasonal storage change of tundra ponds in a polar oasis environment. *Permafrost and Periglacial Processes*, Vol. 17, pp. 309-323.
Woo MK, Young KL (2006) High arctic wetlands: their occurrence, hydrological characteristics and sustainability. *Journal of Hydrology,* **320**, 432-450.
Woo MK, Young KL, Brown L (2006) High arctic patchy wetlands: hydrologic variability and their sustainability. *Physical Geography,* **27**, 297-307.
Yoshikawa K, Hinzman L (2003) Shrinking thermokarst ponds and groundwater dynamics in discontinuous permafrost near Council, Alaska. *Permafrost and Periglacial Processes,* **14**, 151-160.
Young KL (2006) Assessment of snow storage and ground ice melt in high arctic environments. *Hydrological Processes,* **20**, 2643-2645.
Zhang T, Stammes K (1998) Impact of climate factors on the active layer and permafrost at Barrow, Alaska. *Permafrost and Periglacial Processes,* **9**, 229-246.
Zona D, Oechel W (2008) The Biocomplexity manipulation experiment: effect of water table drop on CH_4 and CO_2 fluxes in the Alaskan Arctic at the Barrow Environmental Observatory. In: *Ninth International Conference on Permafrost*, Vol. Abstract (ed Kane D. HKM). Institute of Northern Engineering, Fairbanks, Alaska.
Zona D, Oechel WC, Kochendorfer J, Paw U KT, Salyuk AN, Olivas PC, Oberbauer SF (2009) Methane fluxes during the initiation of a large-scale water table manipulation experiment in the alaskan arctic tundra. *Global Biogeochemical Cycles,* **23**,

Curriculum Vita

Edith Jaurrieta de Velasco was born in El Paso, Texas to Julio Jaurrieta and Ignacia Prieto de Jaurrieta. She graduated from Socorro High School in 1990 and attended the University of Texas at El Paso (UTEP) with a full engineering scholarship. Edith left UTEP after one semester and moved to Austin, Texas. She pursued Engineering at Austin Community College and the University of Texas at Austin. Unfortunately, part-time employment and a major car accident made engineering studies difficult. She switched majors and pursued English and Sociology, attaining a double major Bachelor of Liberal Arts Degree in December 1998.

Edith briefly worked for the IRS in Austin, but moved to Portland, Oregon and became a family and youth advocate for the Oregon Council for Hispanic Advancement. After almost three years of working and traveling throughout Oregon, Edith left Portland and moved back to El Paso, Texas to pursue an environmental career. She enrolled in the Environmental Science Program and participated in many summer internships, including the Smithsonian Biodiversity and Conservation Program in Virginia (2003), and the Research Experience for Undergraduates in Svalbard, Norway (2004). She was awarded "Best Environmental Science Poster" at the Geological Sciences Colloquium in 2005 for her research in Svalbard. Upon graduation, Edith was awarded the "Best Environmental Science Researcher" by the Environmental Science Program, and earned a Bachelor of Science degree in December 2005. By January 2006, Edith was enrolled in the Environmental Science Masters Program at UTEP.

Edith married Dr. Aaron Velasco in May 2006 and immediately started a family, which put a hault on graduate school. As of September 2007, Edith was back as a mom and graduate student at UTEP. Since her comeback, Edith has co-authored two publications outside of her studies:

- A.A. Velasco and **E. Jaurrieta de Velasco**, 2010. *Striving to Diversify the Geosciences Workforce.* EOS 91: 33, 289-290.

- G. A. Cordero, S. A. Farinas, L. E. McGee, L. Reed, **E. J. Velasco**, R. Rino, C. L. Glenn, and C. Wong, 2008. *Voices of Hope in a Rapidly Changing World*. ESA Bulletin 89: 3, 245-249.

Edith is currently the treasurer and memberships chair for the SEEDS Network of Alumni and Professionals. She is hoping to help bring awareness to other underrepresented minorities (URM) about careers in science, especially geosciences, ecology, and environmental science. She also volunteers at the Insights El Paso Science Museum as education committee co-chair and exhibits committee member. Edith wants to give back to her community and raise interest in science careers. There is much work ahead of her.

Permanent address: 833 Tepic Drive
El Paso, Texas 79912

This thesis was typed by Edith Jaurrieta de Velasco.